



UvA-DARE (Digital Academic Repository)

Nonlinear dynamics of epileptic seizures on basis of intracranial EEG recordings

Pijn, J.P.; Velis, D.N.; van der Heyden, M.; de Goede, J.; van Veelen, C.W.M.

DOI

[10.1007/BF01464480](https://doi.org/10.1007/BF01464480)

Publication date

1997

Published in

Brain Topography

[Link to publication](#)

Citation for published version (APA):

Pijn, J. P., Velis, D. N., van der Heyden, M., de Goede, J., & van Veelen, C. W. M. (1997). Nonlinear dynamics of epileptic seizures on basis of intracranial EEG recordings. *Brain Topography*, 9, 249-270. <https://doi.org/10.1007/BF01464480>

General rights

It is not permitted to download or to forward/distribute the text or part of it without the consent of the author(s) and/or copyright holder(s), other than for strictly personal, individual use, unless the work is under an open content license (like Creative Commons).

Disclaimer/Complaints regulations

If you believe that digital publication of certain material infringes any of your rights or (privacy) interests, please let the Library know, stating your reasons. In case of a legitimate complaint, the Library will make the material inaccessible and/or remove it from the website. Please Ask the Library: <https://uba.uva.nl/en/contact>, or a letter to: Library of the University of Amsterdam, Secretariat, P.O. Box 19185, 1000 GD Amsterdam, The Netherlands. You will be contacted as soon as possible.

Nonlinear Dynamics of Epileptic Seizures on Basis of Intracranial EEG Recordings

Jan Pieter M. Pijn*, Demetrios N. Velis*, Marcel J. van der Heyden#, Jaap DeGoede#, Cees W.M. van Veelen[§], and Fernando H. Lopes da Silva*[^]

Summary: **Purpose:** An understanding of the principles governing the behavior of complex neuronal networks, in particular their capability of generating epileptic seizures implies the characterization of the conditions under which a transition from the interictal to the ictal state takes place. Signal analysis methods derived from the theory of nonlinear dynamics provide new tools to characterize the behavior of such networks, and are particularly relevant for the analysis of epileptiform activity. **Methods:** We calculated the correlation dimension, tested for irreversibility, and made recurrence plots of EEG signals recorded intracranially both during interictal and ictal states in temporal lobe epilepsy patients who were surgical candidates. **Results:** Epileptic seizure activity often, but not always, emerges as a low-dimensional oscillation. In general, the seizure behaves as a nonstationary phenomenon during which both phases of low and high complexity may occur. Nevertheless a low dimension may be found mainly in the zone of ictal onset and nearby structures. Both the zone of ictal onset and the pattern of propagation of seizure activity in the brain could be identified using this type of analysis. Furthermore, the results obtained were in close agreement with visual inspection of the EEG records. **Conclusions:** Application of these mathematical tools provides novel insights into the spatio-temporal dynamics of "epileptic brain states". In this way it may be of practical use in the localization of an epileptogenic region in the brain, and thus be of assistance in the presurgical evaluation of patients with localization-related epilepsy.

Key words: Chaos; Nonlinear dynamics; Intracranial EEG; Temporal lobe epilepsy; Ictal propagation.

Introduction

Nonlinear dynamical theory, sometimes colloquially called "chaos theory", offers the possibility to unveil, on the basis of a single (EEG) signal, dynamical

properties of the system generating that signal. The investigator may thus look at differences in the dynamics of a neuronal network during normal activity as well as in the course of an epileptic seizure. Since one may assume that the generation of ictal activity in the brain corresponds with a specific dynamical state (or set of states) which is/are different from normal ongoing activity, nonlinear dynamical analysis of EEG signals provides an interesting mathematical tool to detect and characterize such state(s).

Babloyanz and Destexhe (1986) were the first to describe a special type of ictal activity in terms of nonlinear dynamics. They estimated the correlation dimension (D_2) and the largest Lyapunov exponent of an EEG of an absence seizure. They reported a considerably lower value of the correlation dimension for seizure activity than for normal activity while a positive value was estimated for the largest Lyapunov exponent. These results indicated that the EEG of an absence seizure was of a low dimensional chaotic nature. Iasemidis et al. (1990, 1994, 1996) described a drop in the value of the largest Lyapunov exponent at seizure onset in temporal lobe epilepsy (TLE), with small time differences in the exact moment of decrease for different recording derivations (subdural ECoG recordings of the left latero-temporal region of the brain).

*Instituut voor Epilepsiebestrijding, "Meer en Bosch" / "De Cruquishoeve", Heemstede, The Netherlands.

#Department of Physiology, State University Leiden, Leiden, The Netherlands.

§Department of Neurosurgery, University Hospital Utrecht, Utrecht, The Netherlands.

^Graduate School of Neurosciences, Institute of Neurobiology, Faculty of Biology, University of Amsterdam, Amsterdam, The Netherlands.

Accepted for publication: April 20, 1997.

We thank Tjeerd olde Scheper for his help in doing the analyses and Wouter Blanes for his continuous support in producing code for our computer as well as text for this manuscript. This work was subsidized in part by CLEO (Dutch Commission for research in Epilepsy), grants A71 and A88, by the NEF (Dutch Epilepsy Foundation), grant 95-01 and by NWO (Netherlands Organization for Scientific Research), grant 629-61-270. Parts of this work have been presented at the 1994 Annual Meeting of the American Epilepsy Society.

Correspondence and reprint requests should be addressed to Dr. J.P.M. Pijn, Instituut voor Epilepsiebestrijding, "Meer en Bosch" / "de Cruquishoeve", Achterweg 5, 2103 SW Heemstede, The Netherlands.

Fax: +31-(0)23-5294324

E-mail: pijn@dds.nl

Copyright © 1997 Human Sciences Press, Inc.

In an earlier study (Pijn et al. 1991) we were able to demonstrate a very clear decrease of the value of the correlation dimension occurring at seizure onset in a well-controlled experimental animal model of epilepsy (limbic kindling in the rat). The drop in the value of D_2 was most pronounced in the "focal area" while the process of spread of seizure activity could be followed by computing D_2 for various brain areas, using intracerebral electrodes, at a distance from the "focal area". We compared, for the first time, the D_2 values with those of corresponding surrogate (randomized) signals and found conspicuous differences for the ictal EEGs.

Frank et al. (1990) and Theiler (1995) have analyzed partly overlapping ictal EEG from the same data set (scalp recording). Theiler concluded that he failed to find clear low values for D_2 : the results were hardly different from those obtained using randomized signals.

On the contrary, Lehnertz and Elger (1995) found low values for the correlation dimension for intracranially recorded ictal signals. They did a correlation dimension analysis on EEGs of 20 patients with unilateral temporal lobe epilepsy (TLE). A clear gradual decrease in D_2 was found during the seizures, most pronounced in the so-called "zone of ictal onset". Furthermore, they found episodes of a decreased D_2 in the interictal EEG allowing an exact lateralization of the primary epileptogenic area.

When performing a correlation dimension analysis it is implicitly assumed that the signal to be investigated is stationary. The onset of an epileptic seizure is, however, intrinsically a nonstationary phenomenon. This implies that, strictly speaking, D_2 analysis should not be applied to signals from brain areas where a transition to epileptic seizure activity takes place.

Nevertheless, in practice, a D_2 analysis may give valuable information as an operational measure when it is applied to overlapping short EEG epochs (a sliding window) that encompass the transition to seizure activity. Various aspects have to be taken into consideration in the case of a transition (which is, of course, nonstationary) (Havstad and Ehlers 1989). In Appendix B we show, for a particular example how such a transition may influence the D_2 value. The relative insensitivity of D_2 for parts of the epoch containing different dynamics allows the use of D_2 in practice for the analysis of the whole (nonstationary) seizure by applying a sliding window approach.

We have investigated intracranially recorded EEGs obtained from a group of 5 patients undergoing preoperative evaluation for intractable complex partial seizures (CPS) of temporal origin (MTLE). In these patients conventional methods sufficed both for identification of the so-called "zone of ictal onset" and for the pattern of ictal

activity propagating to other areas in order to have consistent reference material. For this group of patients we compared the value of various nonlinear measures (stationarity, time reversibility, coarse grained D_2 and entropy K_2) of pre-ictal and ictal signals recorded both in the epileptogenic focus and far away from it (van der Heyden et al. 1996, van der Heyden personal communication).

In the present study we concentrated on the evolution of one of these measures, D_2 , during various types of activity and during transitions between these types of activity. We analyzed in one patient interictal spiking, pre-ictal activity, seizure onset, propagation of seizure activity throughout the brain and the progression of a seizure from its earliest states until its end. Detailed D_2 analyses were performed by means of a step-by-step analysis of signals recorded in the zone of ictal onset (right pes hippocampi), its contralateral homologous area and signals recorded in the temporal neocortical areas of both hemispheres.

Material and Methods

The EEG

The patient

The EEG segments analyzed were from a 30 year old female with medically intractable MTLE. She was investigated with invasive EEG/video telemetry according to the protocol described by Van Veelen et al. (1990). A total of twelve subdural reeds and four intracerebral bundles were introduced. Subchronic electrocorticography and stereoencephalography (SCECoG & SEEG) identified focal seizure onsets in the right pes hippocampi during partial seizures with elementary symptomatology (auras of rising epigastric sensation) as well as during clinically invalidating partial seizures with complex symptomatology (CPS). EEG segments analyzed included pre- as well as ictal signals obtained bilaterally from the anterior-, mid- and posterior lateral temporal convexity as well as from the pes hippocampi and the amygdala.

Recording of the EEG

Multiple subdural reeds bundles and miniaturized multi-contact depth electrodes (manufactured by Brain Electronics BV, De Bilt, The Netherlands) were introduced in a combined procedure bilaterally and more or less symmetrically. Subdural electrodes covered extensive areas of the fronto-orbital, frontolateral and lateral- as well as sub-temporal neocortical areas of both hemispheres. In addition a limited number of intracerebral multi-electrode bundles were implanted stereotactically

in the anterior part of the pes hippocampi and in one or both amygdalae according to the coordinates described in the atlas of Delmas and Pertuiset (1959). Both subdural and intracerebral electrodes were introduced through two symmetrical parasagittally located frontal trephine openings.

Interictal and ictal intracranial EEG was acquired using Braintronics pre-amplifiers (Braintronics B.V., Almere, The Netherlands) with a bandwidth of 0.16 - 100 Hz (3 dB points, 6 dB/octave), sampled and digitized by a custom-made 21 channel Pulse Code Modulated (PCM) cable telemetry system at a frequency of 366.2 Hz and continuously recorded on paper while selected sections and all clinical seizures were also recorded digitally on a VME computer (Plessey Microsystems/Radstone Technology plc., England). The monopolar EEGs were recorded with respect to G1, which is a submastoidal scalp electrode. The potential of G1 was kept on a constant level, equal to the potential of the outer surface of a small box (containing pre-amplifiers, ADC and PCM-encoder) carried in a vest pocket worn by the patient; the potential was kept constant by inducing a current in another scalp electrode, G2, placed close to G1. Patient behavior was continuously recorded by video stored on Super VHS videotape.

Use of a rather low value for the high-pass filtering (0.16 Hz) for the pre-amplifiers allowed for the detection of very slow potentials at the beginning of the seizure. Such slow potentials may be ascribed to increases in extra-cellular potassium concentrations as described by Wadman et al. (1992). These slow potentials correspond with very broad autocorrelation functions. Calculation of D_2 for these data would require, therefore, the use of a very large window T for the "Theiler correction", leaving an insufficient number of vectors for a reliable estimation of D_2 . When a fixed, moderately sized value, is used for T (150 ms) for the analysis of these data, "false" low D_2 's are obtained at high values of $\log(r)$. Since we are primarily interested in the dynamics of the fast electrical activities, we performed all further analyses by first digitally high-pass filtering the data (using an autoregressive FIR filter consisting of 1000 terms constructed using the program MATLAB (MathWorks Inc., Natick, MA, U.S.A.)).

The Mathematical Tools

Calculation of D_2

The correlation dimension was determined according to the following procedure: The EEG signal was sampled as a discrete time-series: x_0, x_1, \dots, x_{N+k} . Assuming that the dynamics of the system generating the signal occupies an attractor A , it is a generic property that the set of N vectors:

$$\vec{V}_m(i) = (x_{i+k_0}, x_{i+k_1}, x_{i+k_2}, \dots, x_{i+k_{m-1}}), \quad (1)$$

$$(0 \leq k_l \leq k, l = 0, \dots, m-1)$$

forms an embedding, provided, $m > 2D(A)$ with $D(A)$ the dimension of the submanifold containing the attractor A (Takens 1981). According to Grassberger and Procaccia (1983) the correlation dimension can be calculated by first determining the correlation integral $C(r, m)$:

$$C(r, m) = \frac{1}{N^2} \sum_{i=1}^{N-W} \sum_{j=i+W}^N h(r - d(\vec{V}_m(i), \vec{V}_m(j))) \quad (2)$$

in which h is the Heaviside or step function ($h(x < 0) = 0$, $h(x \geq 0) = 1$) and d the distance between two vectors (we use the maximum norm: the largest absolute difference between corresponding components).

Grassberger and Procaccia used $W = 1$. In order to avoid spurious dimensions due to autocorrelation in a time series Theiler (1986) suggested to exclude from the calculation of (2) all vectors the corresponding coordinates of which are correlated. This can be done by using a window $W > 1$. For a sampling frequency v , the length of the window is in time domain equal to $T = W/v$. Theiler suggested taking T equal to the "the autocorrelation time" of the signal. In the present study, for the analysis of the patients signals, we used a fixed value for T (150 ms, justified in Appendix A).

The following step in determining the correlation dimension D_2 is to assume that, within a range of values of r (usually called the scaling region), the following relationship holds:

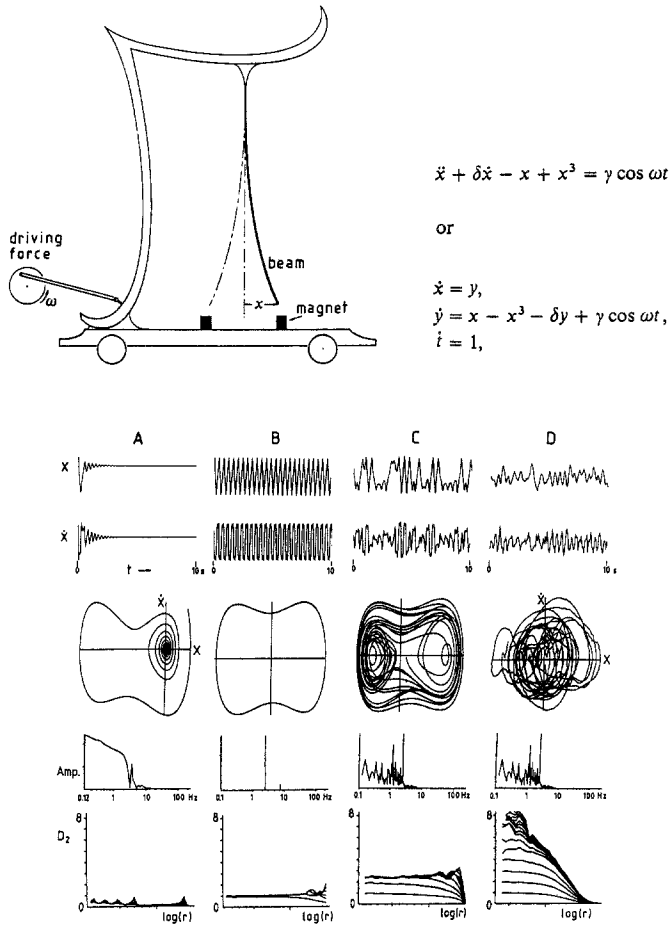
$$C(r, m) \sim r^{D_2} \quad (3)$$

for m large enough.

A numerical value for D_2 is sometimes determined by (i) calculating $C(r, m)$ for a high value of m (in the range between 15 and 20), (ii) choosing a value of r and then taking the local slope of $\log(C(r, m))$ versus $\log(r)$ as estimate of D_2 . This estimate is called the "coarse grained" estimate of D_2 .

More often a region of r -values is considered for which $\log(C(r, m))$ behaves as a linear function of $\log(r)$. This range of r -values is called the "scaling region". Usually, the slope of a line fitted through the points $(\log(r), \log(C(r, m)))$ within the scaling region is used as the value of D_2 .

These methods give an approximation of D_2 . In case of EEG data, however, the scaling region is mostly rather narrow and limited to large values of r . Therefore, it is particularly important to report the range of values of r



for which D_2 is determined.

We chose to present the complete relationship by means of the plot of the local slope of $\log(C(r,m))$ versus $\log(r)$ instead of presenting only one value of D_2 for a given signal (We calculated the local slope by taking the difference between successive values of $C(r,m)$.) In case a plateau is present in a D_2 -plot the corresponding estimate of D_2 may be simply read from the corresponding value on the ordinate axis. Furthermore, should a plateau be present only for a limited or narrow range of values of r , then the D_2 -plot gives information about the dependence of D_2 on the various parts of the signal corresponding to different amplitudes (i.e., large-amplitude epileptiform spike-and-wave complexes versus low-amplitude background EEG).

In figure 1 we present three examples of D_2 -plots, one for a transient, another for a limit cycle and a third for chaotic dynamics, each of them generated by the Duffing equation (Guckenheimer and Holmes 1983). This figure illustrates that for long signals (16000 samples) D_2 -plots may be obtained with clear plateaus at the correct level (zero, one and a value between two and three, respectively, for the transient, limit cycle and the chaotic dynamics described with the three first-order differential equations). Figure 1D shows the D_2 -plot of surrogate data of the same length.

We were obliged to use much shorter epochs for the

Figure 1. Demonstration of different types of dynamical behavior of the Duffing equation (one second order differential equation or a set of three first-order differential equations). The Duffing equation is a good description of the behavior of a metal beam above two magnets. The term $\delta\dot{x}$ expresses the friction. $-x + x^3$ describes the attractive forces of the magnets on the beam, while $\gamma \cos \omega t$ is an external driving force. Signals A, B and C are solutions of the equation. In A $g=0$, therefore, the beam settles itself close to one of the magnets. In phase space (third row), this is expressed as a point attractor. $D_2 \approx 0$ for such transient behavior (fifth row). In B and C, $g = 0.3$, $w = 1$, and $d = 0.15$. Now (B and C) the external force pumps in energy. Therefore, stationary behavior becomes possible. Given the values of g , w and d either limit cycle (B) or chaotic (C) behavior is possible depending on the initial conditions only (i.e., the starting point of the beam). Limit cycle behavior occurs for a starting points outside the region of the magnets, while chaotic behavior occurs when the tip of the beam is left free in-between the magnets.

For signals A and B $x = 1.6081$, $\dot{x} = 0.8783$ and $t = 0.773$ (precisely on the limit cycle). For C $x = 0.5$, $\dot{x} = 0.5$ and $t = 0$. The limit cycle gives D_2 while chaotic behavior yields $2 < D_2 < 3$, which corresponds to a set of three first order differential equations.

The signals in D were made by randomizing the phase angles of the signals in C. Both signals in C and D have the same amplitude spectra (fourth row from the top). The D_2 plot in the case of the surrogate signal (D) does not show the plateau seen for the chaotic signal (C).

The spectra and D_2 calculations were carried out for the signals presented in the first row from the top. For A, however, the epoch analyzed had a length of 2,500 samples (half the length shown), while for B, C and D the epochs analyzed consisted of 16,000 samples (3.2 times the length shown) (for the time axis, we considered the sampling rate to be 500 Hz). The range of the abscissa of the D_2 -plots is a factor 29.1. This figure is adapted from Lopes da Silva et al. (1996).

analysis of the real EEG signals because of the nonstationarity of these signals as already mentioned. Nevertheless, even the epochs we used (10 seconds, 3662 samples) were often not quite stationary: the signals often changed gradually in character during the epoch and sometimes also in amplitude. Therefore D_2 -plots as "pure" as those of figure 1 could not be expected for the real EEG signals. Notwithstanding the above, some of the D_2 -plots obtained from the real data showed plateaus at similar levels as those in figure 1, corresponding to similar types of dynamics.

Reconstruction parameters

(a) We used 10 seconds (3662 samples) for the length of the epochs. (b) We used delays (k values), for the reconstruction (1) in phase space, homogeneously distributed between 20 and 300 ms with embedding dimensions from 1 up to and including 17. (c) We used $T=150$ ms for the 'Theiler correction'. (d) We used autoscaling for the abscissa of the D_2 -plots (a pilot study taught us that seizure spread was best expressed by changes in D_2 -plots on this way). The autoscaling was done identically for all D_2 -plots shown. We used the following procedure. The largest r occurring between all reconstructed vectors was chosen as the highest value on the abscissa, $C(r,m)$ were calculated for 33 radii, chosen in such a way that successive radii had a ratio of 0.9 (the ratio between the largest and the smallest radius is, therefore, $(0.9)^{-32} = 29.1$). This means that we 'looked' at the data with an amplitude window having an upper boundary equal to the maximal distance between all vectors (since we used the maximum norm this equals the maximal difference in amplitude between all samples within the epoch) and a lower boundary which is 29.1 times smaller than the upper boundary.

Comparison with surrogate data

We compared the D_2 -plot of the EEG signal with that of a corresponding surrogate signal to find out whether a D_2 -plot (or of a plateau in such a curve) is merely due to a combination of an arbitrary choice of delays and of the spectral properties inherent to the EEG signal or it truly reflects nonlinear properties of the dynamics of the system generating that signal. Various authors have introduced and applied this method independently in order to identify non-random structure in a time series. An elaborate introduction of the method is given by Theiler et al. (1992A), while a summary of the history of the method and a demonstration of its usefulness and limitations may be found in Rapp et al. (1993). We have demonstrated the necessity of using it in order to avoid misinterpretations, especially in the case of normal and epileptiform EEGs (Pijn 1990; Pijn et al. 1991).

Surrogate data can be constructed in various ways

(Theiler et al. 1992A). Theiler et al. (1992B) introduced the terms "algorithm-zero, -one and -two surrogates". We used algorithm-one surrogate signals (as we did before in Pijn et al. 1991). Such signals are constructed to yield a random signal which has the same spectral properties as the original time series and Gaussian amplitude distribution (e.g., signal D in figure 1).

Interpretation of the results of a D_2 analysis

If no apparent difference in D_2 -plots is obtained between the original and an algorithm-one surrogate signal one must conclude that the original signal cannot be distinguished from a linear Gaussian random signal by means of a D_2 analysis (Theiler et al. 1992A; Takens 1993). Differences will be found between surrogate-one and original signals if:

1. the signal-generating process is a linear stochastic process having a non-Gaussian amplitude distribution (Rapp et al. 1994) or if
2. the signal-generating process is of a low-dimensional (non-linear) deterministic nature or if
3. the recording system (read-out function) introduces non-linearities. Non-linear transformations might occur at the electrodes and/or in the EEG registration equipment, e.g., by digital filtering.

A discussion arose in recent years as to which type of surrogate test should best be used (Osborne et al. 1986, Osborne and Provenzale 1989, Theiler et al. 1992A, Theiler et al. 1992B, Kaplan and Glass 1992, Provenzale et al. 1992, Kaboudan 1993, Rapp et al. 1993, Rapp et al. 1994, Muhlnickel et al. 1994, Prichard and Theiler 1994, Kantz and Schreiber 1995, Theiler and Rapp 1996).

Although this controversy is not yet settled, we consider that, in the case of an epileptic oscillation we could be allowed to interpret **prominent** differences in D_2 between an original signal (low value) and its corresponding surrogate (large value) as evidence of the existence of a low-dimensional order. This means that a considerable degree of determinism is present in the system generating the signal.

Test of reversibility

An alternative method to assess the nonlinear structure of a signal is to test whether the time series is reversible or not. A time series is said to be reversible only if its probabilistic properties are invariant with respect to time reversal. Diks et al. (1995) have proposed a test for the null hypothesis that a time series is reversible. Rejection of the null hypothesis implies that the time series cannot be described by a linear Gaussian random process (LGRP) or by a static transformation of a LGRP. This test was applied in the present work and more elaborately on similar type of signals by van der Heyden et al. (1996).

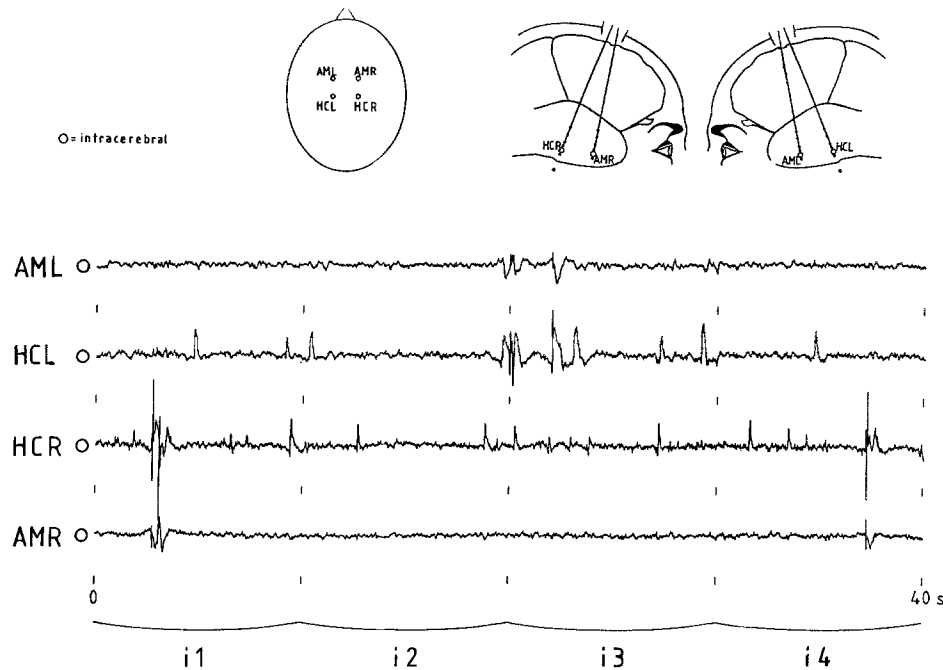


Figure 2. Forty seconds of interictal EEG, recorded three minutes before seizure onset. AML = amygdala left, HCL = hippocampus left, HCR = hippocampus right, AMR = amygdala right. Four 10-seconds-long epochs were analyzed. These epochs are denoted i1-i4.

Recurrence plots

As stated earlier, the onset of an epileptic seizure is a transition (and therefore nonstationary) expressed by a change in character of the EEG signal. A way of investigating such a transition is to make a recurrence plot of the signal. Such plots were introduced by Eckmann et al. (1987) and are based on the following. As the behavior of a nonstationary system changes from one mode to another the distance between any vector (constructed according to equation (1)) of the first mode and a vector of the second mode will become relatively large, when compared with the distances between any two vectors belonging to one and the same mode. Therefore, it is possible to visualize the occurrence of transitions in the behavior of a system and to distinguish different modes of operation. We used the following method to make a recurrence plot. The time index i in (1) was represented running from the first to the N^{th} sample along both axes. A point was plotted for each pair of indices (i, j) at position (i, j) , if the distance in m -dimensional space between the vectors $\vec{V}_m(i)$ and $\vec{V}_m(j)$ was smaller than a fixed threshold. Consequently, apparent "grayness" of the final plot depends on the value of such a threshold. However, such plots do not change substantially for quite a range of threshold changes. An illustrative example is given in Appendix C.

Results

Interictal activity

We analyzed two interictal periods. The first period consisted of a 40-seconds-long EEG segment which occurred three minutes before seizure onset. Since epileptiform activity was only present in the hippocampi and amygdalae during this period we analyzed just those channels. The corresponding EEG signals are shown in figure 2. Four successive epochs each lasting 10 seconds were analyzed. The epochs were coded with an "i" to denote interictal activity. The second period of interictal activity occurred just before the seizure. It consisted of three epochs of 10 seconds each. The epochs were coded with a "P" (pre-ictal activity) while the corresponding EEG is shown in figure 4.

During both interictal periods D_2 analysis yielded almost identical plots for the original and surrogate signals for all signals in which epileptiform spikes were not present: left amygdala (AML) during i1 and i4, right amygdala (AMR) during i2 and i3 and all electrodes in the left hemisphere and the right temporal electrodes in the pre-ictal episode (figure 3). All the other signals containing epileptiform spikes yielded very low D_2 levels in the high amplitude range, most of them about zero. This corresponds with the very low level in the D_2 -plot shown in figure 1A, which is due to the presence of a

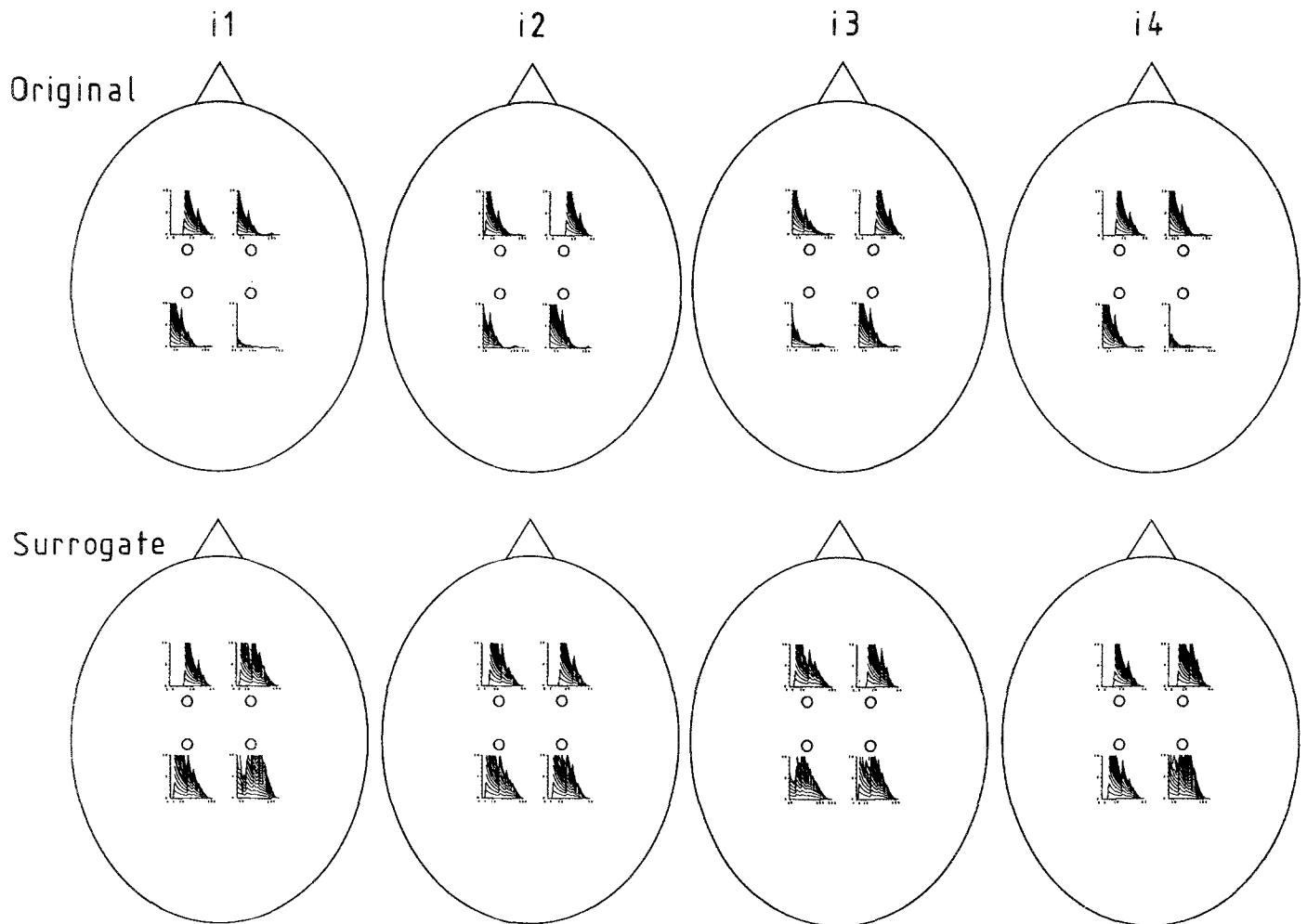


Figure 3. Results of D_2 analysis of the signals in figure 2. The right tip of the abscissa of each D_2 -plot corresponds with the largest difference between all amplitudes of the samples of the epoch. The range of the ordinate of each D_2 -plot is from 0 to 10. The numbers i1-i4 correspond with the epochs as denoted in figure 2.

transient. A low level somewhat different from zero was obtained for HCL during i3 and a level clearly different from zero for HCR during P3. During these latter epochs the spikes were more grouped together than during those that yielded a zero value for D_2 .

Seizure onset and spread

The seizure may be described as having a Type B pattern of onset according to Townsend III and Engel Jr (1991) characterized by hypersynchronous high-voltage, low-frequency spikes in the HCR channel. This pattern is followed by a period of very fast, low-voltage activity. Although we did not have access to the orbitofrontal regions in our EEG record, the time relationship of the sequential involvement of the contralateral hippocampus is consistent with the findings of Lieb et al. (1991), group 1, pattern 2 of seizure spread: right mesial temporal onset of seizure discharges followed by invasion of

the right orbitofrontal region, then the left orbitofrontal region and finally the left mesial temporal structures some 20 seconds (according to their figure 5) after seizure onset.

Figure 4 displays the EEG of our patient around seizure onset as recorded by a selection of 10 intracranial electrodes out of a total of 21 recorded ones. The choice of channels displayed was made on the basis of the signals which best illustrated the characteristics of the group 1, pattern 2 seizure spread. The high-voltage, low-frequency spikes of seizure onset are prominent at second 30 of figure 4 in the channel recording from the right hippocampus (HCR). These spikes accompany the ictal semiology of a partial seizure with elementary symptomatology (rising epigastric sensation). Approximately 20 seconds later, around second 50, the same EEG-pattern may be seen in the contralateral hippocampus (HCL), expressing the involvement of the left temporal mesial structures in the seizure. From the above it

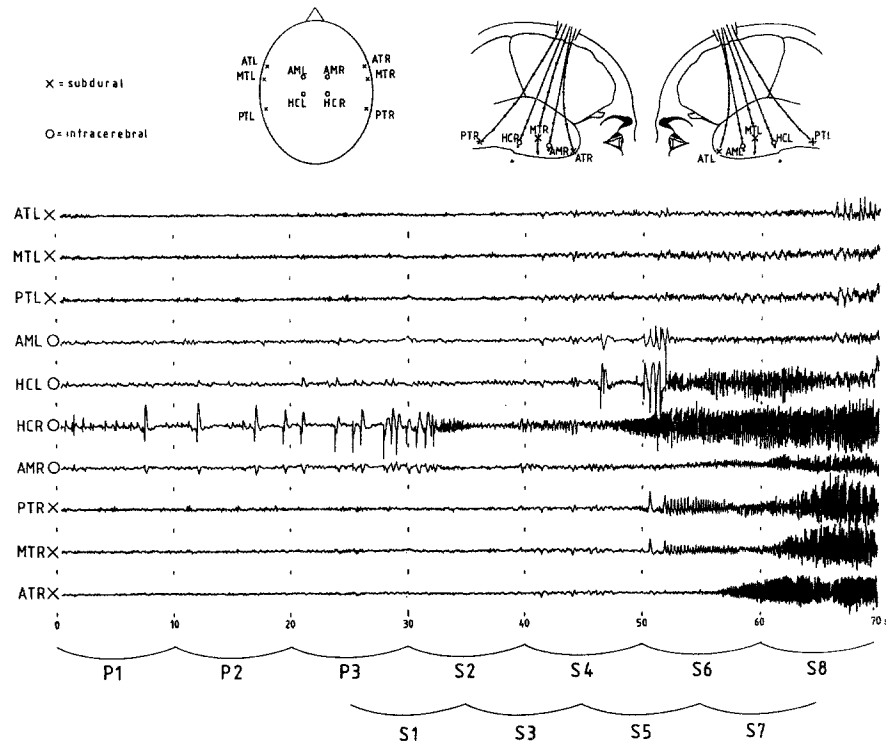


Figure 4. Above: schematic representation of the position of the intracranial electrodes. Below: a 70-second-long EEG including the onset of a complex partial seizure. The tracings derived from the left hemisphere are denoted by abbreviations of the subdural reeds and intracerebral bundles ending in "L", while those from the right hemisphere end in "R", AT = anterior temporal, MT = mid temporal, PT = posterior temporal, AM = amygdala, HC = hippocampus. Epochs P1 through to P3 display pre-ictal signals with interictal spikes present HCR and AMR. Seizure onset occurs around second 30 (epoch S1) in HCR (right hippocampus) expressed by hypersynchronous high-voltage, low-frequency spikes, followed by a period of very fast, low-voltage activity. Around second 50 (epoch S5), a similar EEG-pattern may be seen in the contralateral hippocampus (HCL). From that time onwards ictal activity 'fans out' to PTR, MTR and ATR (and during S8 to ATL) suggesting propagation to the basal and lateral temporal neocortex ipsilaterally (and later contralaterally). At that moment the seizure becomes partial complex. Two sets of epochs were analyzed: one pre-ictal set denoted P1-P3, and a second set, during seizure onset of half overlapping epochs denoted as S1-S8.

may be clear that we are not implying that the seizure propagates *directly* from one hippocampus to the other. Furthermore, we see in figure 4 ictal activity propagating 'outwards' to the basal and lateral temporal neocortex first ipsilaterally and somewhat later contralaterally. At that moment the patient became unresponsive (the seizure became complex partial). The pattern of ictal propagation (from second 50 onwards) classifies this seizure as one of type A in table 4 of Brekelmans et al. (1995): a temporal mesiolimbic seizure according to its pattern of chronological ictal involvement.

Analyses of seizure onset and spread

We used 10-second-long epochs with a 50% overlap in order to follow the process of seizure onset with a high time resolution. The epochs are denoted as S1 up to and including S8 in figure 4 while the result of the analysis is shown in figures 6 and 7 for the original and surrogate

signals respectively.

Although practically all epochs S1-S8 contain some channels showing manifest ictal activity which can readily be identified by any experienced EEGer, the corresponding D_2 -plots do present a real challenge. In some epochs and for some channels the D_2 -plot of the original signals hardly differ from those of their respective surrogate signals. On first examination one quickly tends to be baffled by the variety and the variability of the plots obtained.

One should, therefore, perform a sequential comparison of the EEG signals and of the corresponding D_2 -plots keeping in mind that the variability of the signals as the seizure evolves should be represented by specific patterns of changes in the D_2 -plots. Reciprocally, the variability of the D_2 -plots themselves should make it imperative to look for presence of particular graphoelements in the EEG signals. Indeed, by doing this we observed that by sequential comparison from signal to D_2 -plot and back again the D_2 -plots function as a sort of

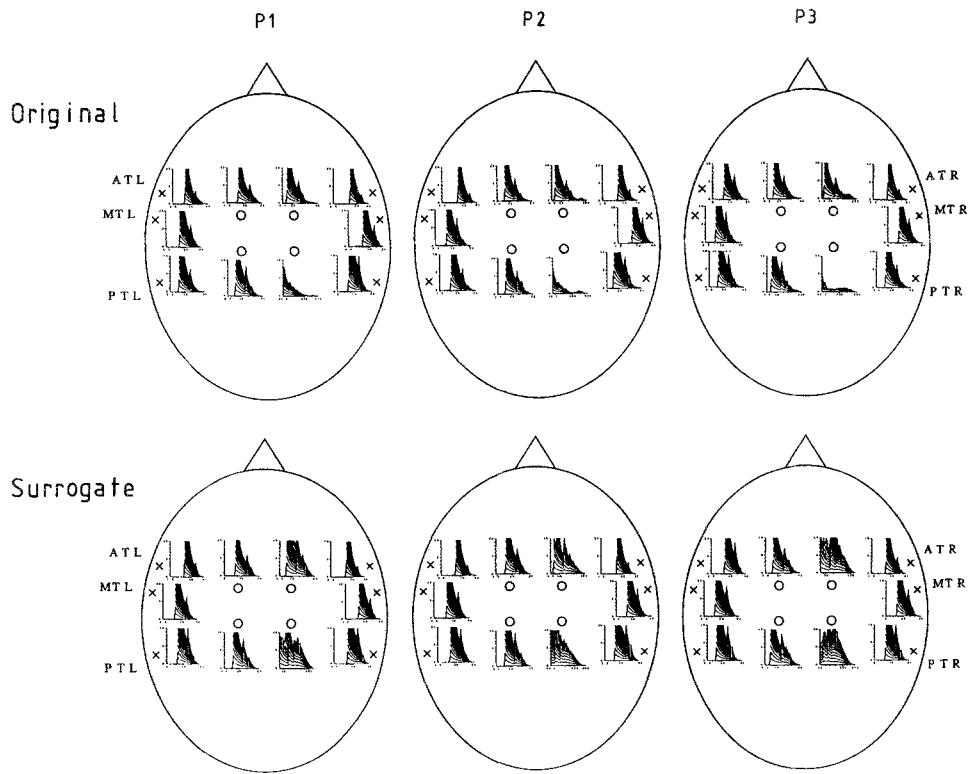


Figure 5. Results of D_2 analysis of signals and their surrogates, corresponding with epochs P1-P3 in figure 4.

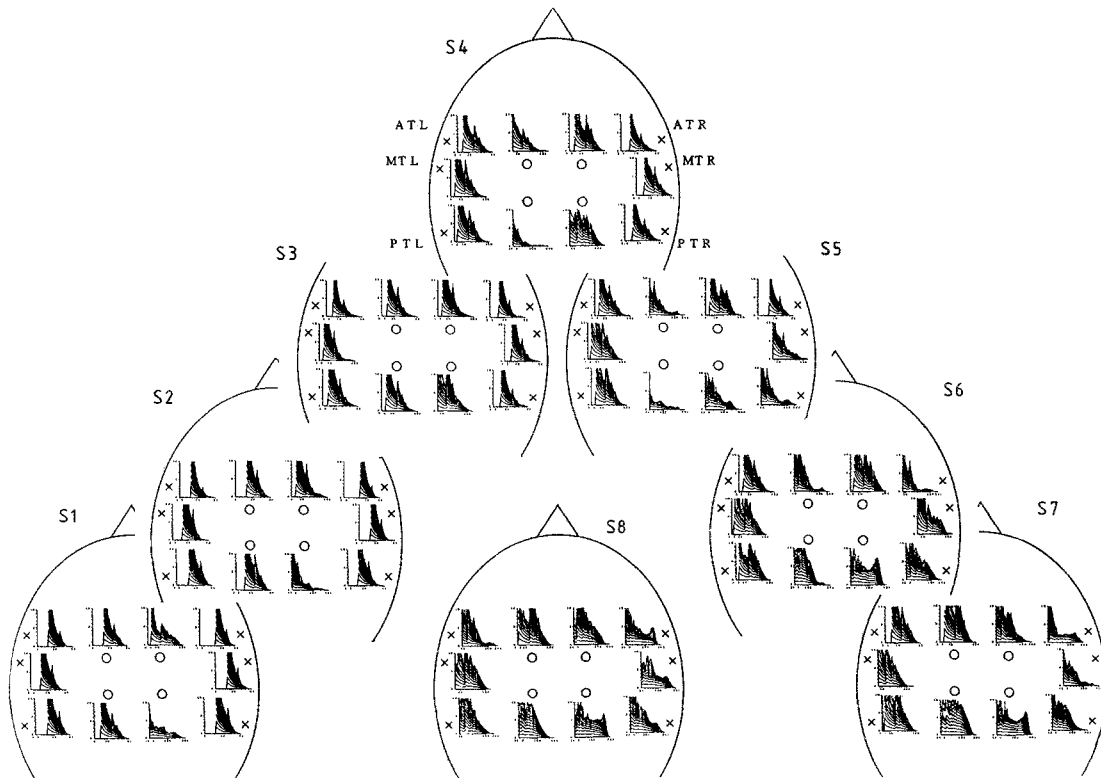


Figure 6. D_2 -plots of the signals in figure 4, epochs S1-S8.

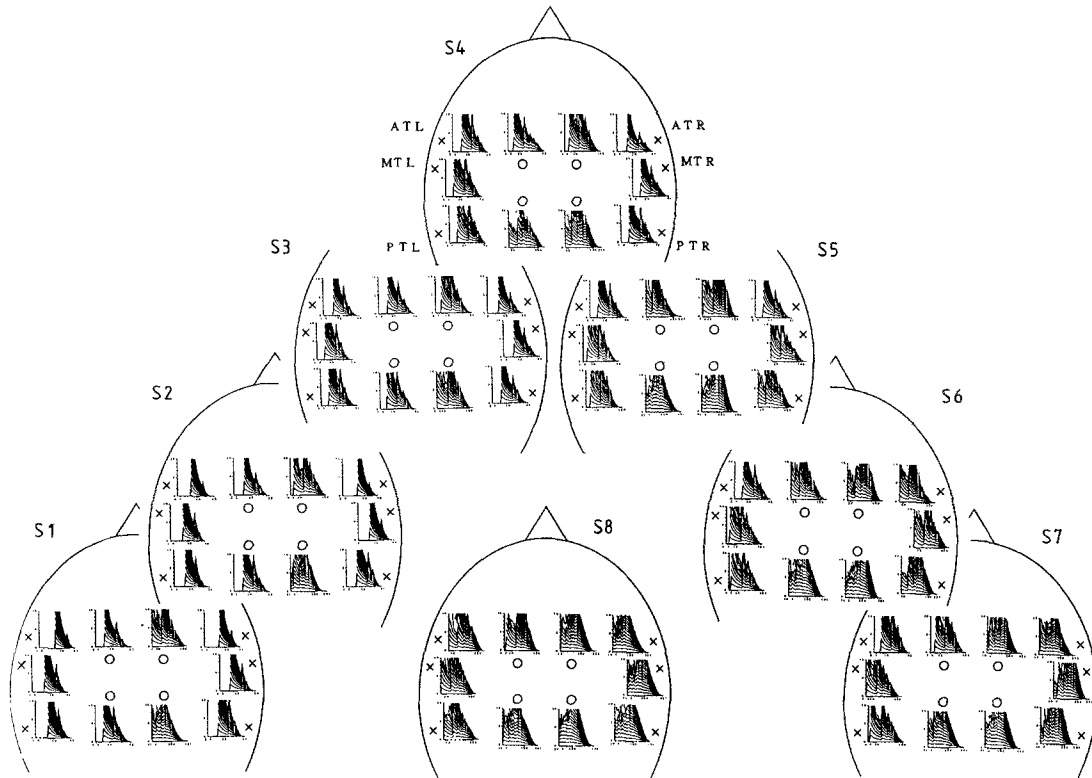
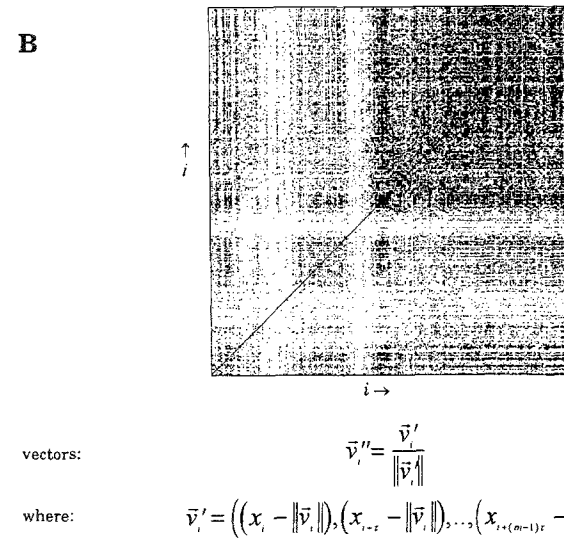
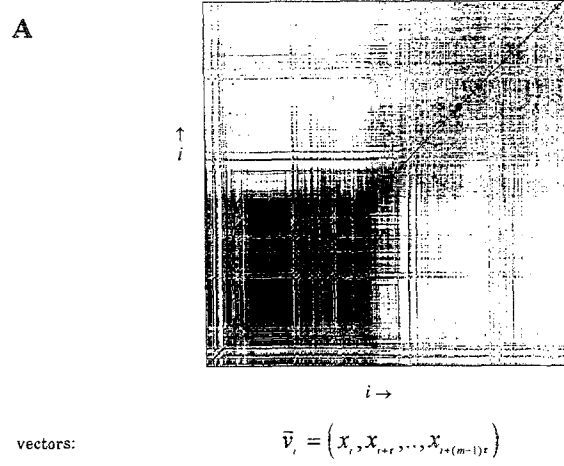
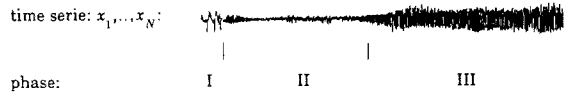


Figure 7. D_2 -plots of the surrogate signals corresponding with the signals in figure 4, S1-S8.

magnifying glass, revealing information in the original EEG signal which might otherwise have been overlooked. Systematic sequential comparison of signals, D_2 -plots and electroclinical correlations in this case did allow us to distinguish four periods in the evolution and spread of the seizure:

- i. Focal onset: This period shows a definite similarity with the pre-ictal period (P-epochs) in which the D_2 -plots of the HCR and AMR were approximately zero (during P1 and P2). Subsequently a gradual increase of the D_2 -plot levels is noted. This is more pronounced during S1 than during P3 both for the HCR and AMR. Although the D_2 -plot levels in S1 are clearly different from zero they are also clearly different from the corresponding surrogates. These intermediate levels for HCR and AMR during S1 no longer correspond to the presence of isolated large amplitude transients in the signals but rather suggest the presence of low-dimensional dynamics for the group of spikes occurring in the middle of S1. During S2 the levels decrease again. The D_2 -plots of HCR shows a plateau close to zero, while, that of the AMR shows almost zero-values only for large amplitude spikes (note that this epoch covers only a part of the above mentioned group of spikes).
- ii. Transitional dynamics: during S3 the D_2 -plot of HCR differs clearly from the preceding one by having larger D_2 -plot values and no longer showing a clear-

cut plateau. The same holds true for the AMR going from S3 to S4. During S4 the differences between the D_2 -plots of the original and surrogate signals from the HCR and AMR become very small. The increase in D_2 -plot values could be due to either very complex dynamics or to nonstationary behavior. One should realize that a nonstationarity such as a transition from a low-dimensional process to another low-dimensional one does not induce a large D_2 value (Appendix). However, a sequence of many short-lasting processes with different dynamics within a single epoch may present a random character and should, therefore, yield a large D_2 . In order to find out whether the HCR signal during S3 and S4 presents nonstationary behavior we made recurrence plots of this signal. Figure 8 shows HCR signal recurrence plots during epochs S2-S8. Epochs S3 and S4 correspond with phase II in figure 8. If a signal is stationary its recurrence plot is homogeneous. During phase II, however, the recurrence plot is only partially homogeneous. Signals that contain a transition from one type of dynamics to another one which is disjunct in phase space from the preceding one have white off-diagonal squares in their recurrence plots (an example is given in the Appendix). Since this is not found in figure 8 for phase II, we may conclude that this type of nonstationarity does not occur during phase II. Nevertheless, various stripes are visible in the recurrence plot during phase II. Since these



stripes indicate the presence of (nonstationary) transients, we may reject the conclusion that phase II is stationary.

- iii. Spread to the contralateral mesial temporal structures: at the same time as the dynamics of HCR show a transition to high values, the signals of the contralateral hippocampus HCL present a D_2 -plot first of a level zero (S4), corresponding with the presence of a large-amplitude spike, and then, during S5, with a plateau indicating low-dimensional dynamics of the same type as initially was present in HCR.
- iv. "Generalization": This period coincides with ictal involvement of both temporal lobes. Note that the D_2 -plots not only do reflect spread to contra-lateral hippocampus (in S5) but also spread to the temporal areas as well (from S5 onwards for the right hemisphere, while spread to the left temporal neocortical region is apparent only during S8 by a low level plateau for ATL). In general, epochs S5-S8 show a complex set of D_2 -plots, some with (almost) zero level D_2 plateaus and others with low-level D_2 plateaus in the range between 2 and 5. Plateaus of approximately value 3 are found for ATL during S7 and for all three temporal neocortical areas on the right during S8. HCR's D_2 -plots during S6-S8 show a clear plateau at a level approximately equal to 4 and, therefore, are clearly different from the previous ones. This suggests the presence of a different dynamics during S6-S8 than previously. This suggestion is confirmed by the recurrence plot of figure 8A. The figure shows a dramatic separation between the sectors corresponding to phases I and II and to phase III with primary white off-diagonal areas. This means that during phase III a different volume of phase space is occupied than during I and II. It may be noticed, however, that during phase III the amplitude (variance) of the signal increases considerably with respect to phase II. The question arises whether the difference between II

Figure 8. Recurrence plots of the time series shown in the upper trace (signal from HCL, second 30-70 in figure 4). Three successive phases marked I, II and III may be distinguished.

The 'normal' recurrence plot, comparing vectors \vec{v}_i with vectors \vec{v}_j (as described in Appendix C) is shown in 8A. The three different phases in the signal (time domain) may also be recognized as such in the recurrence plot (phase space). The large amplitude epileptiform spikes in phase I are reflected as empty horizontal and vertical stripes across the whole plot. Such stripes emerge in a recurrence plot at short lasting events that are disjunct in phase space to the rest of the signal, thus at transients. Phase II shows a pattern that is relatively filled, with some stripes. Both phases I and II appear to form one block, indicating that the dynamics of signals occur in one and the same area of phase space. However, Phase III consists of a clearly different pattern, i.e., of a grayish area with two relatively empty areas around it (the off-diagonal squares). Therefore phase III reflects dynamics in phase space which are disjunct from those of phases I and II. In B vectors \vec{v}_i'' are compared with vectors \vec{v}_j'' . These vectors are derived from the original signal by correcting the original vectors \vec{v}_i and \vec{v}_j for first- and second-order nonstationary changes in the signal (respectively in the mean and the variance of the signal), consequently losing two dimensions of the embedding: one because one of the components of \vec{v}_i'' is equal to zero (as well as the same component in \vec{v}_j'') and another one because all vectors \vec{v}_i'' have a length equal to 1. Vectors \vec{v}_i'' form a projection of the original trajectories on a hypersphere having two dimensions less than the original embedding space.

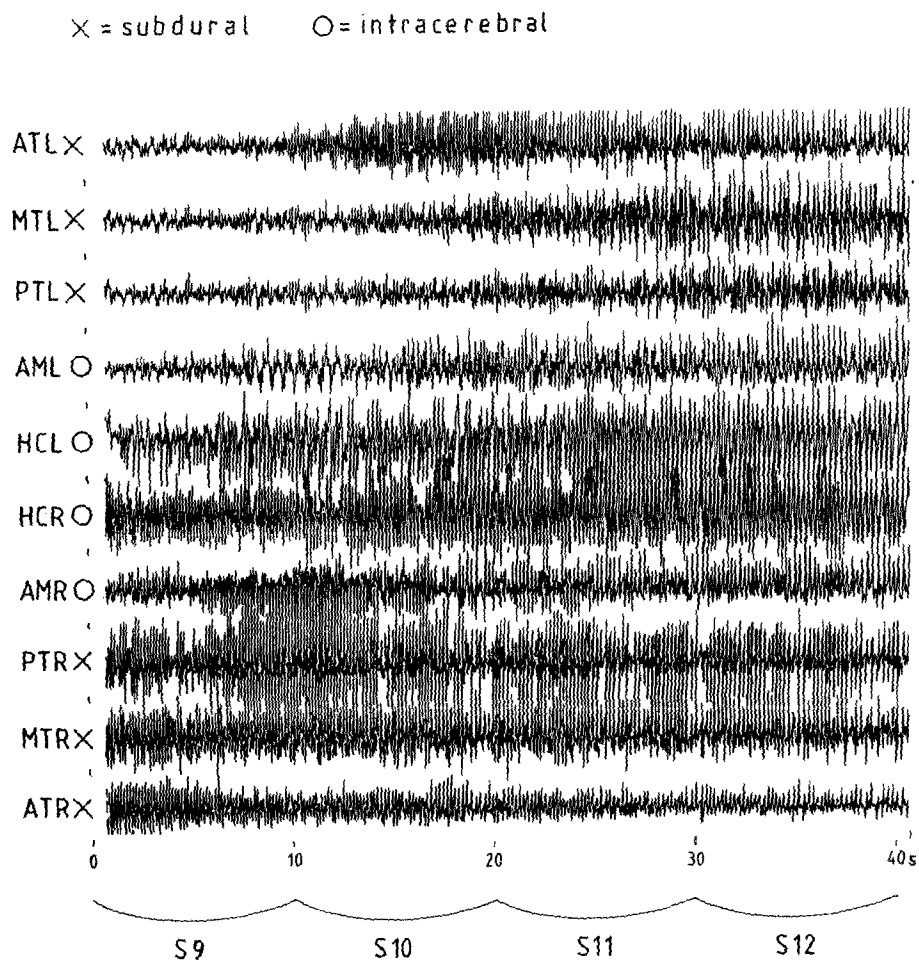


Figure 9. Progression of the complex partial seizure. Plots are made for epochs immediately after those in figure 4.

and III is just due to an increased amplitude or really to a difference in dynamics. In order to answer this question we made a recurrence plot (figure 8B) of vectors derived from the original signal by normalizing with respect to the mean and the variance of the signal (in this way a projection of the trajectories on a hypersphere which has two dimensions less than the original embedding space is created). When comparing 8B with 8A it may be noticed that the appearance of the plots changes. The small-amplitude noisy phase II now becomes more "thin" in phase space, because of fewer vectors located closely to each other. The opposite holds true for phase III: the large variation in amplitude of the vectors is reduced bringing them closer together. What is important is that phases II and III can still easily be distinguished in figure 8B. Therefore, we may conclude that at the beginning of phase III (corresponding with second 50 in figure 4) a transition takes place. At that moment a different dynamical process starts. This process has a D_2 in the order of 4, with a D_2 plot clearly different from the one of the corresponding surrogate. This conclusion was

confirmed by applying a reversibility test on the signals of phases II and III. Applying this test yielded no rejection of the null hypothesis for phase II and rejection for phase III, confirming a different behavior of the generating network during these two phases.

Analysis of seizure progress

As shown already in figure 4, the zone of ictal onset (HCR) entered a stage of relative low complexity ($D_2 \approx 4$) with a clear plateau at approximately second 50. This stage lasted some 20 seconds. Two questions may be raised: (i) does this stage persist in the hippocampus for the remainder of the seizure? And (ii): does this type of D_2 -plot "spread" to other brain areas?

In order to answer these questions we extended the analysis to another 40 seconds of EEG immediately following the signals in figure 4. The additional EEG signals and the results of the analysis are shown in figures 9 and 10 respectively. As far as the first question is concerned, we confirm the D_2 -plots of the original sig-

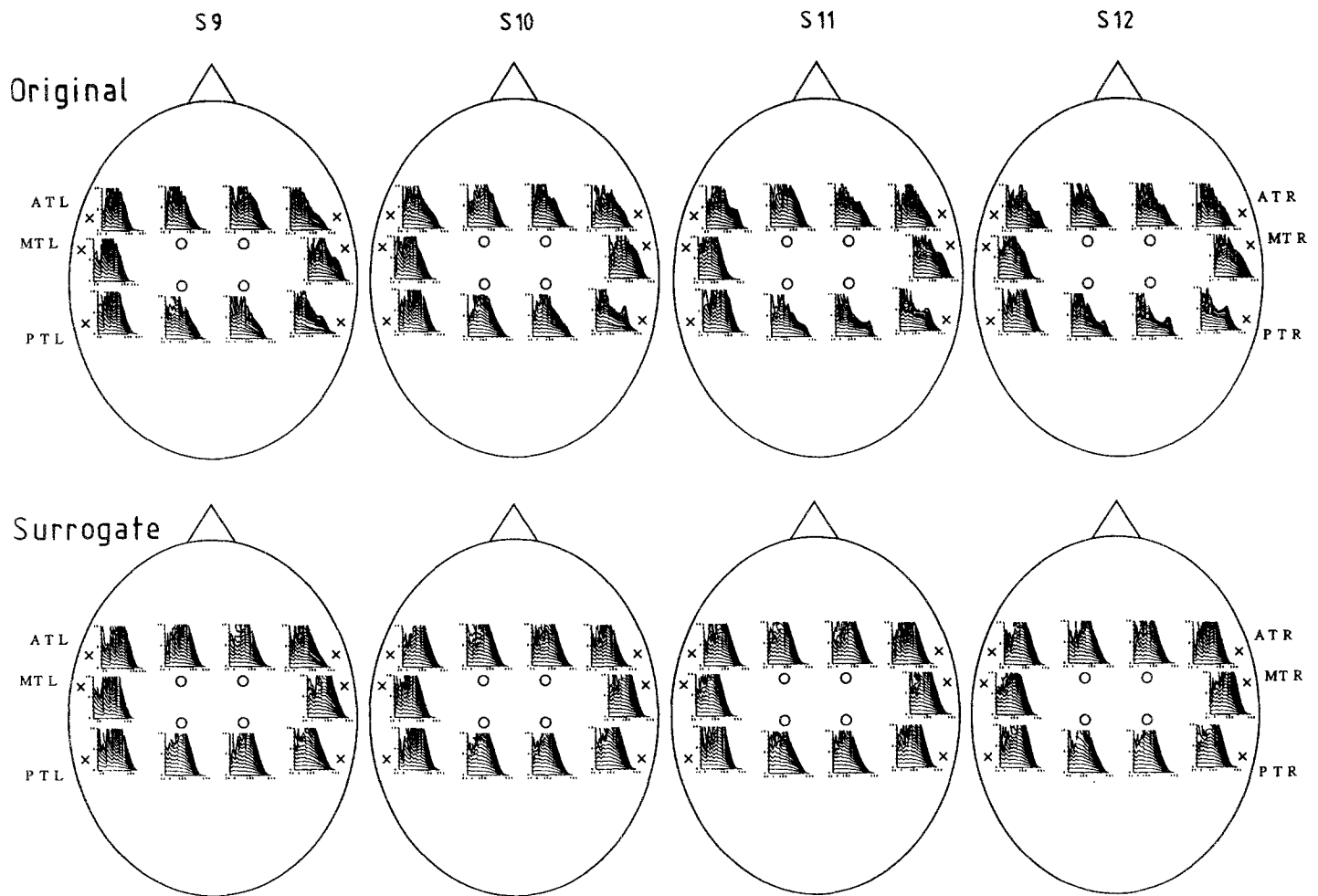


Figure 10. Results of analysis of the signals in figure 9.

nals are different from their corresponding surrogates during S9 and S10. However, a plateau in the D_2 -plot of HCR is no longer present for these two epochs only and reappears during epochs S11 and S12 for the duration of the seizure. Regarding the question of " D_2 -plot spread" we found the HCR type D_2 -plots (i.e., those of epochs S6-S8) for PTR, and, to a lesser extent, for MTR, during epochs S9 through S12.

It may be argued that our results of the D_2 -plots might have been affected by "contamination" through the reference electrode or by activity from other brain regions, in particular during the "generalized" phase of the seizure. To rule out such "contamination" we performed subsequent analysis using bipolar derivations, constructed from nearby contact pairs of each hippocampal bundle. We were therefore able to compare the results of a referential montage with those of a bipolar one for signals derived from the same contacts covering the same areas of the brain, including the zone of ictal onset and the zone of primary ictal spread in order to estimate the extent of 'noisy' artificial influence in signals recorded

with the reference montage.

The bipolar signals for the hippocampal bundles HCR and HCL and the D_2 -plots obtained using these derivations are shown in figure 11. The D_2 -plots of the corresponding monopolar derivations were shown in figures 5 (epochs P1-P3), 6 (epochs S1-S8) and 10 (epochs S9-S12).

We note that the differences between D_2 -plots of the monopolar and bipolar signals are negligible from epoch P1 up to and including epoch S9. However, in epochs S11 and S12 differences between the monopolar and bipolar D_2 -plots are more evident with more pronounced plateaus for the bipolar ones, particularly for HCL. Reviewing the patient's time-locked video recording corresponding with these epochs confirmed presence of gross motor unrest (temporal seizure automatisms). We conclude that the monopolar signals might have been contaminated by a high-dimensional process, most likely 'noisy' movement artifacts (caused by movements of the miniaturized cable telemetry PCM encoder and preamps in the patient's vest pocket as she thrashed about wildly

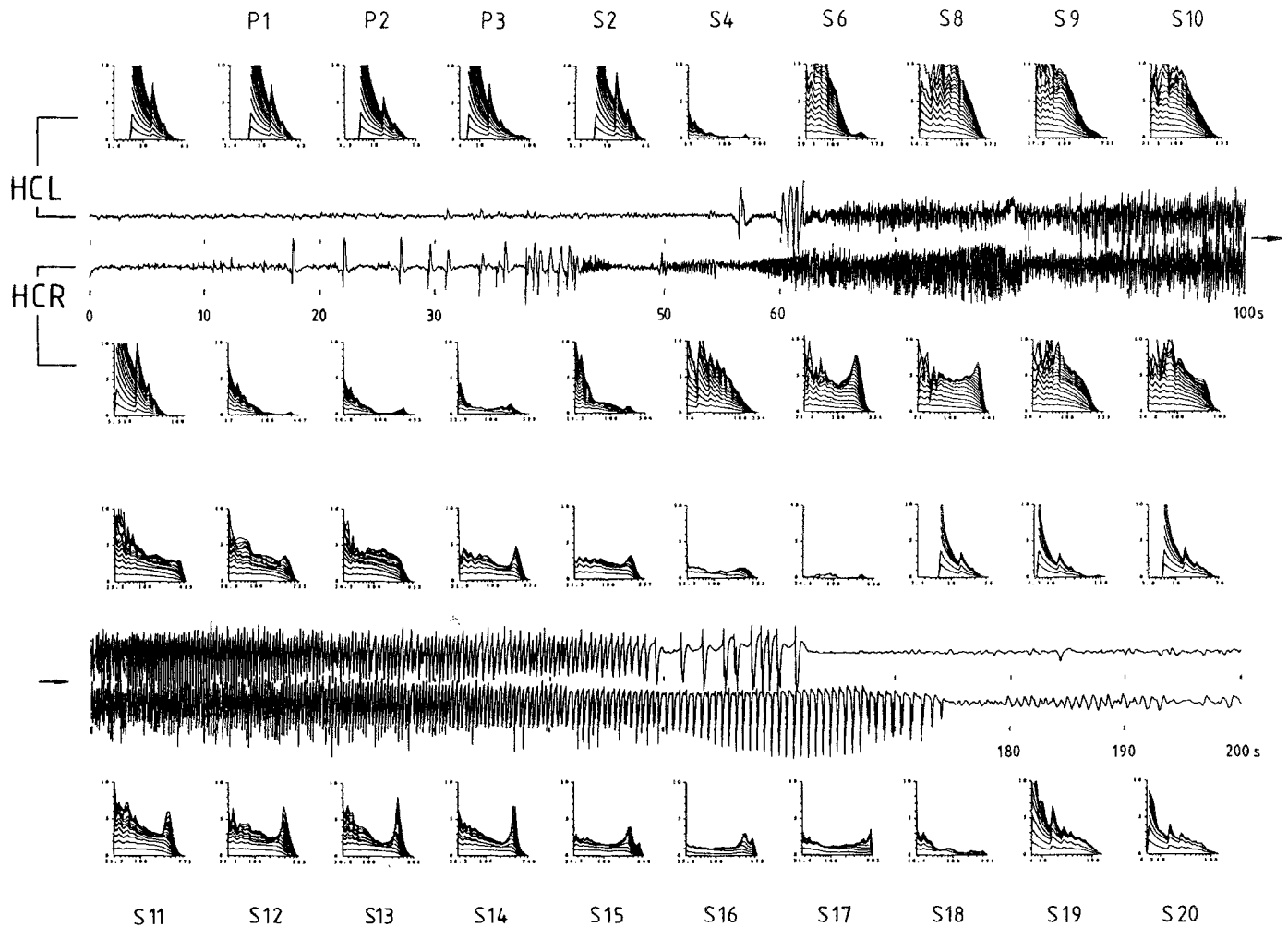


Figure 11. Bipolar derivations and corresponding D_2 -plots of signals recorded in both hippocampi during the pre-ictal phase (epochs P1-P3), the complete seizure (S2-S18) and a part of the post-ictal phase (S19-S20). D_2 -plots obtained using these signals are shown for successive 10-seconds-lasting epochs.

at the time), and that this contamination could be avoided using bipolar recordings.

Therefore, the low-dimensional stage emerging at second 60 in figure 11 (second 50 in figure 4) in the zone of ictal onset, HCR, is rather persistent: it is present during almost the remainder of the seizure, with the exception of the 20 seconds of epochs S9 and S10. Furthermore, a possible noisy artifact in the reference electrode may have hidden the emergence of clear low-dimensional plateaus in the D_2 -plots during the ictal spread to the lateral temporal neocortical areas.

It is obvious that the low-dimensional state does 'spread' from the ipsilateral hippocampus to the contralateral one: a clear low dimensional plateau emerges and persists in the D_2 -plots of the contralateral hippocampus from approximately second 100 (figure 11) onwards. Strangely enough this low-dimensional state in the left hippocampus is reached a full 40 seconds after seizure

activity became present in that brain area. Last but not least, the further the seizure progresses (from S11 onwards) the lower the values in the D_2 -plots of the two hippocampi, until the seizure stops (just before second 180).

Discussion

Several caveats apply in discussing the present study in view of related literature. To begin with, our results were based upon three episodes during one SCE-CoG & SEEG record in a single case of MTLE. Although electrophysiologically and clinically speaking the results of the D_2 -plots obtained make perfect sense in this case, it would be inappropriate to extend them to other cases of MTLE. Even though D_2 -plot analysis in this case did yield excellent results in terms of delineating the epileptogenic zone as well as paralleling ictal spread through-

out the brain, we note that the situation might be quite different, even for intracranial recordings, in cases of extratemporal localization-related epilepsy which we and others still expect that shall need implantation of intracranial electrodes in the future. Both the use and the usefulness of this type of detailed analysis might, therefore, prove quite limited. Certainly, when it comes to automatic seizure detection, other techniques of QEEG analysis are more efficient, economical and readily available (Gotman 1982, 1990).

In contrast to others (Iasemidis et al. 1994 and 1996, using Lyapunov exponents) we have not been able to ascribe any value to the D_2 -plots in predicting the onslaught of a complex partial seizure. In fact our results suggest that the dynamics in the zone of ictal onset might be too complex in the interictal, pre-ictal and early ictal phase in this case and that behavior reminiscent of a low-dimensional chaotic attractor becomes manifest in a consistent way only well into the seizure.

In the present study we have shown that:

- i. Activity of the reference electrode may be of considerable influence on the D_2 -plots. Bipolar montage reconstructing are the method of choice while, in case of monopolar recordings, one should take care with interpreting high values for D_2 in ruling out extraneous 'noisy' contamination through the reference electrode.
- ii. Furthermore, we demonstrated that all signals that did not show clear epileptiform activity always yielded a D_2 -plot hardly distinguishable or even identical to their corresponding surrogate signals, regardless of whether they were sampled during the interictal, pre-ictal or ictal epochs analyzed. We found a striking influence of large-amplitude epileptiform spikes on D_2 -plots. Interictal signals containing such spikes always yielded a very low D_2 , close to zero. Large-amplitude spikes had a marked effect on the D_2 -plots in epochs which consisted of primarily low-voltage activity, as is usually the case for interictal EEG. This is 'trivial' since any sharp transient in a signal causes such a result. The background (non-epileptiform) activity can be considered as a point attractor with respect to the spike. We expect others (Lehnertz and Elger 1995) have not noticed such an influence of interictal spikes because of the way they extracted D_2 values from their D_2 -plots, i.e., by essentially "filtering out" large-amplitude spikes.
- iii. Finally we demonstrated that signals showing seizure activity always yielded a D_2 -plot different from surrogate. However, the differences varied from being subtle to very large (with the presence of a clear plateau). Indeed there was a marked degree of non-stationarity in most of the signals during the course of the seizure. Therefore, it is inappropriate to consider a single value for D_2 for the whole of this type of seizure and thus only an analysis that takes into

account the evolution of D_2 in the course of time might reveal the whole truth. Recurrence plots were useful in this respect.

These conclusions merit further discussion.

Ongoing non-epileptiform activity

Although many investigators have considered the possibility that dynamical processes in the brain are of a low-dimensional chaotic nature (among others: Skarda and Freeman 1987; Babloyantz and Destexhe 1986; Freeman 1995), such has never reliably been proven for "normal" on-going brain activity (it was shown by Hayashi and Ishizuka 1995, and Ishizuka and Hayashi 1996 that EEG signals may be chaotic. These signals, however, were not spontaneously occurring signals but evoked by stimulating afferent fibers). To our knowledge ongoing EEG in most cases does not yield a value of D_2 that differs clearly from surrogate signals. Nevertheless, various authors have reported statistically significant differences between D_2 values of EEGs recorded during the performance of different mental tasks and/or between 'normal' control EEGs and EEGs recorded during various pathological brain states (reviewed in Pritchard and Duke 1992, Pradhan and Narayana Dutt 1993 and Elbert et al. 1994).

Authors who have investigated differences between D_2 's of original 'normal' EEG and corresponding surrogate signals report different results. Practically no difference could be demonstrated for EEGs recorded (i) in a rat sitting quietly and during explorative behavior (Pijn 1990; Pijn et al. 1991), (ii) during the human monosynaptic spinal cord stretch reflex (Hoffmann reflex, electromyographic recording of the gastrocnemius muscle) (Schiff and Chang 1992), (iii) during an all-night sleep of a human subject (Achermann et al. 1994), (iv) during relaxation with eyes closed (Palus 1992; Pritchard and Theiler 1994) and (v) during rest or during the performance of a simple mental task (counting) with eyes closed (Theiler and Rapp 1996). However, Soong and Stuart (1989), Cerf et al. (1994) and Rombouts et al. (1995) reported a difference between D_2 's of original 'normal' EEG (alpha rhythm) and corresponding surrogate signals. Recently, Müller-Gerking et al. (1996) and Pezard et al. (1996) reported weak evidence of nonlinear dynamics in data recorded from the visual system (of cats, pigeons and humans). All differences reported are subtle, much smaller than can be observed for seizure activity. Blińska and Malinowski (1991) and Hernández et al. (1995), who considered the predictability of alpha rhythm, also report quite different results for different scalp EEG recordings. In Lopes da Silva et al. (in press) we have discussed the 'randomness' of alpha rhythm in more detail and shown that nonlinear low-dimensional oscillatory alpha activity may occur in the form of short bursts.

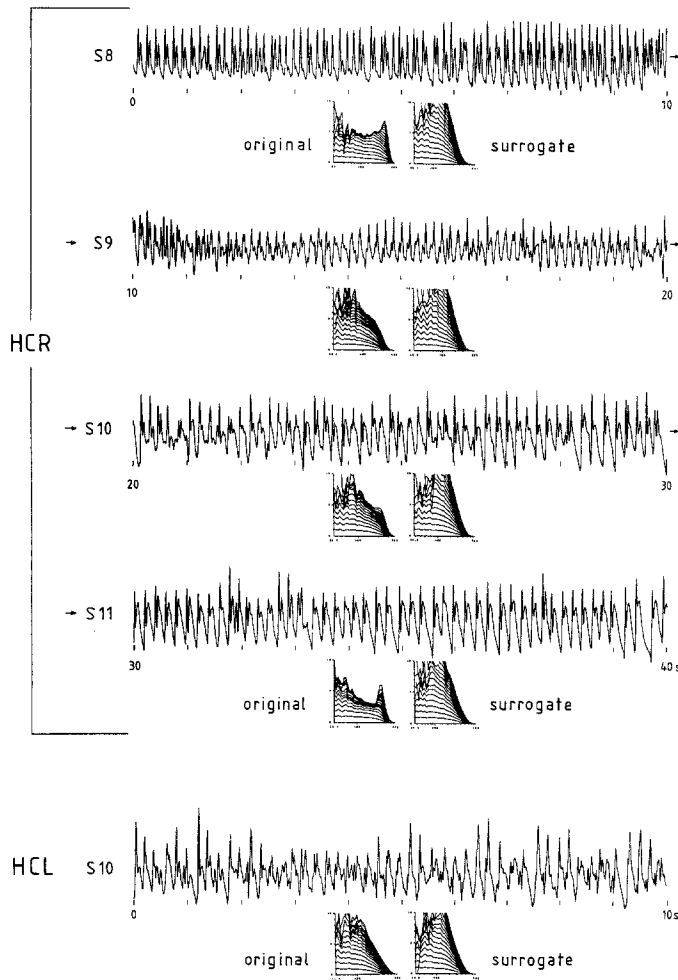


Figure 12. A selection of EEG signals from figure 11 (bipolar derivation), presented on an enlarged time scale together with their corresponding D_2 -plots. The arrows denote the continuation of the EEG for concatenated epochs. Furthermore, the D_2 -plots of the corresponding surrogate signals are shown.

Epileptiform transients, interictal EEG

We know of no report in the literature specifically addressing the effect of interictal spikes on D_2 calculations. Lehnertz and Elger (1995) reported regularly occurring episodes of a relative decrease in D_2 in interictal EEG, which is more pronounced in the zone of ictal onset, but they state that such decreases are not due to the presence of spikes.

A difference between this study and ours was that the range of values of r which we used in the D_2 -plots included larger values ($-4.8 \leq \log_2 r \leq 0$) than those used by Lehnertz and Elger ($-5.5 \leq \log_2 r \leq -2.5$). This may lead to a manifest effect of interictal spikes on D_2 -plots in signals such as ours when very large amplitude spikes in relation to the background are present intermittently.

Ictal EEG

As far as ictal EEG in man is concerned only Lehnertz and Elger (1995) and our group have investigated the evolution of D_2 during a complex partial seizure. Both found that if D_2 becomes low during the seizure such a decrease does not last the whole seizure. Furthermore, we found that D_2 varied considerably during the seizure, even in the zone of ictal onset. On the other hand, Lehnertz and Elger explicitly showed a unidirectional change of D_2 during a seizure in what they call the "focal area". A single minimum of D_2 was reached gradually and rather slowly; several minutes after seizure onset. We chose to use rather short epochs with a 50% overlap allowing us to follow the evolution of D_2 with a high temporal resolution. In this way we found that D_2 varies between very high to very low values in the zone of ictal onset with abrupt changes between different stages that take place: within 5 or 10 seconds. We failed to detect uniformly unidirectional changes of D_2 in any area of the brain in the course of the seizure analyzed, although some of the lowest D_2 values appeared to occur during "plateauing" in both hippocampi during the last stage of the seizure (figure 11). Recently we analyzed in five patients with mesial temporal lobe epilepsy signals recorded in the area of seizure onset and compared results of epochs recorded prior to and during the seizure. We found that D_2 (using a 'coarse grained' estimate) is systematically lower during the seizure than prior to it (van der Heyden personal communication).

Seizure onset: a bifurcation in dynamics

Both our results and those of others who dealt with ictal EEG records, therefore point in the same direction: a change in D_2 to low values may be found in the zone of ictal onset and neighboring structures. This finding suggests that there is a change in dynamics at the initiation of an epileptic seizure. This may correspond to a bifurcation in the dynamics of the underlying neuronal network as discussed in more theoretical terms by Lopes da Silva and Pijn (1995). The question becomes one of semantics, i.e., defining "seizure onset". In our case we have defined "seizure onset" to coincide with the appearance of large amplitude hypersynchronous spikes in HCR which make way for low-voltage, fast spike activity as seen in epoch S1 of figure 4.

Seizure progression

The evolution of seizure activity in HCR clearly yields quite different D_2 -plots, as shown in figure 11, while that for HCL parallels HCR with a delay of several seconds until HCL "catches up" with HCR. In figure 12

we show, on an enlarged scale, a number of signals and corresponding D_2 -plots for some epochs in the middle of the seizure. We have selected these epochs because they present marked differences of D_2 -plots (specifically, a difference with surrogates) although, on first impression, the EEG signals appear very similar on visual inspection. However, careful scrutiny of these EEG signals indicates that there are differences in regularity and, furthermore, that the plateauing correlates with the apparent rhythmicity of the signals (while the level of the D_2 -plots shows an inverse correlation with it). It is noteworthy that plateauing of the D_2 -plots occurs at different D_2 levels in one and the same region of the brain (HCR) during consecutive epochs during the seizure.

There appear to be three possible explanations for the above:

- i. One could extrapolate that the dynamics of the system producing the ictal EEG undergoes constant changes which may be expressed by the varying D_2 -plots. We certainly cannot exclude this possibility. In fact, this seems to happen in HCR at second 50 approximately in figure 4, as discussed above. On the other hand, pertaining to the signals of figure 12: all those signals seem to be essentially similar, differences appear to be due more to changes in regularity than to changes in graphoelements. Therefore, it seems not very likely that the signals of figure 12 correspond to different dynamics.
- ii. Alternatively one might be dealing with the effect of a "migrating epicenter" of seizure activity, which might move closer or further away from the fixed recording electrode contact thus yielding apparently different results in the D_2 -plots for one and the same phenomenon, just as one's perception of an atmospheric disturbance might depend upon the vantage point chosen. We consider this explanation not realistic, since we have used bipolar reconstructions of closely spaced hippocampal contacts and, therefore, we have analyzed signals "native" to the hippocampal structures penetrated by these contacts. Regardless whether seizure propagation has occurred elsewhere in the brain, the finding of an ictal signal at any time during the seizure necessarily implies that seizure activity is local.
- iii. Finally, one might consider that the changes noted in the D_2 -plots might be an expression of a variation in the so-called *dynamic noise*. This concept is elucidated by Hammel 1990 and Grassberger et al. 1993. There are different ways by which a dynamic process can be obscured by noise. One of these consists of additive noise. In that case, we consider that from a noise-free sequence of vectors, \vec{V}_i , forming a trajectory for which holds $\vec{V}_{i+1} = f(\vec{V}_i)$, a noisy trajectory is generated by $\vec{V}'_i = \vec{V}_i + n_i$ for small $\|n_i\| < \delta$. The above describes the case where a physical process is

obscured by errors in measurement. Another way by which the dynamics can be obscured by noisy influences is when errors are made upon each iteration of the process. The resulting points of the trajectory satisfy the expression $\|\vec{V}_{i+1} - f(\vec{V}_i)\| < \delta$. This type of error is called dynamic noise. Assuming that seizure activity in a neuronal circuit is generated according to a deterministic rule $\vec{V}_{i+1} = f(\vec{V}_i)$, then other sources of neuronal activity interfering with the seizure activity will act as dynamic noise. This interference may be different in the course of the seizure.

This final explanation is probably the most likely one and we would like to advance the hypothesis of dynamic noise. The (oscillating) hippocampal neurons are widely interconnected (Lopes da Silva et al. 1990) and, therefore, receive continuous input from the rest of the brain (both from the rest of the hippocampus and from extrahippocampal structures). In this respect it is striking that, as shown in figure 11, the final stage of seizure, roughly coinciding with epochs S16 and S17, yields signals consisting almost exclusively of periodic spikes. This suggests that at that time the dynamic noise is minimal, i.e., that we are dealing with a 'pure' oscillation. Given the wide connectivity of the hippocampal structures, this would mean that the input from outside is (almost) absent at that time. One could think of this as a result of spreading depression, exhausting the inputting neurons (notice that shortly thereafter period the epileptic activity in the two hippocampi themselves also dies out).

Conclusion

In this paper we present results which help to confirm, extend and also refute a number of assumptions with respect to the potential use of 'chaos' theory analysis in studying the transition from the interictal to the ictal state. These results were obtained from the analysis of intracranial EEG derived from clinical studies (seizure monitoring in patients with refractory complex partial seizures.)

We were able to offer some indications of valid and potentially helpful use of chaos theory analysis in the study of ictal EEG. It is clear that the choice of montage influences the results of D_2 calculations. Bipolar derivations are to be preferred over monopolar reference ones. While the choice of parameters for the construction of the Takens vectors does seem to influence the details of the calculation it does not have any influence on the interpretation of the dynamics of seizure spread. Therefore, seizure evolution in complex partial seizures may adequately be studied by various methods for

constructing these vectors. We demonstrated that several of these methods (D_2 analysis, recurrence plot, reversibility test) do lead to results which are very similar.

We also demonstrated that a complex partial seizure does not necessarily constitute a single "state of the brain" and that such seizures may not be adequately described by behavior reminiscent of a single, low-dimensional chaotic attractor. What constitutes EEG seizure activity may or may not be accompanied by a plateau of relatively low values for D_2 . The transition from the interictal to the ictal state does not necessarily occur "instantaneously" in spontaneous complex partial seizures. The concept of a single bifurcation to one epileptic state, therefore, seems to be too simplistic in describing the process taking place from the first onset in the 'focal area' to the more or less stable state of a seizure that takes place in a large part of the brain. During the seizure different states seem to occur while, furthermore, the epileptic oscillation seems to be affected by a varying influence of other noisy-like processes (probably from elsewhere in the brain).

It is also quite evident that high voltage sharp transients, have a disproportionately high influence on the outcome of D_2 calculations. Since seizure activity is often accompanied by such sharp transients just before or at the transition to the ictal state it follows that, in these cases, the use of D_2 -plots may be inappropriate as a means of identifying seizure onset. Several other QEEG techniques are currently better suited for and much more efficient in achieving the purpose of automatic seizure detection than computation of D_2 , regardless of an occasional report in the literature of on-line D_2 calculations.

Perhaps the most important of our findings is that calculation of the correlation dimension in complex partial seizures seems to parallel the evolution of seizure activity as it propagates throughout the brain in a way that is in line with the classical clinical neurophysiological interpretation of this phenomenon. While the value of D_2 may vary from site to site as well as in time in partial epilepsy, the so-called zone of ictal onset is invariably identified as that in which the D_2 -plot presents ultimately a stable plateau at a rather low value. As seizure activity spreads to other areas of the brain, intracranial EEG recorded from these sites show also a tendency for the correlation dimension to present a stable plateau, paralleling the sequential involvement of different brain areas in the generation of seizure activity in the EEG. The EEGer engaged in the preoperative evaluation of refractory complex partial seizures will recognize in this technique the potential for analyzing objectively seizure spread, based on seizure dynamics, rather than relying only upon the morphology of the grapho-elements inherent to visual pattern

recognition of epileptiform activity.

Appendices

A: The choice of the delays for the embedding

Although many authors have warned against inappropriate use of reconstruction parameters for the estimation of D_2 and have even provided recipes of what to choose (nicely reviewed by Rapp, 1994), none have published on the influence of parameter choices on the evolution of D_2 during a process of which the dynamics gradually change. In a pilot study we analyzed the spread of an epileptic seizure in a kindled rat brain. We varied the choice of delays and the range of amplitudes in phase space (see r in equation (2), in the text) in various ways and concluded that as long as the parameters are chosen in a reasonable range the exact choice is of very little influence on the expression of seizure spread by means D_2 -plots (Pijn et al. 1992).

In the present study we used, for the reconstruction (1), as smallest/largest value for the k_i 's a value equal to the smallest/largest feature of interest present in the signals (suggested by Takens, personal communication). In epilepsy this corresponds with the duration of (inter)ictal spikes: 20 - 70 ms and the duration of a spike-wave complex: approximately 300 ms (3 per second spike-and-waves).

Apart from the range of the k_i 's one can vary the order of the k_i 's. In the past we used 'independent' delays (Pijn et al. 1991, suggested by van Neerven 1987). This was done as follows. We chose for each embedding dimension all k_i 's as homogeneously as possible distributed over one fixed interval: k_1 =largest value and each following k is chosen such that it was not equal to a previously chosen value but that it has a maximal distance to all of the previous ones (e.g., for $m=10$: $k_i=0, 9, 4, 7, 2, 8, 1, 6, 3, 5$ for $i=0, 1, \dots, 9$). Since the large delays are used for low embeddings the highest curves in the D_2 -plot is reached 'faster' than when using the arithmetic series. Albano et al. 1988 showed already that the crucial parameter is the largest delay used (the length of the window) rather than the value of the highest embedding or the difference between successive delays separately.

Instead of using a fixed range of delays for all signals, it is possible to adjust the range each time again to properties of each particular signal. This is a kind of autoscaling. Usually the range is related to the autocorrelation function of the signal (or the auto-information function as proposed by Fraser and Swinney 1986; additional alternatives are reviewed in Rapp 1994).

We considered the autocorrelation function. Visual assessment of the autocorrelation functions of the ana-

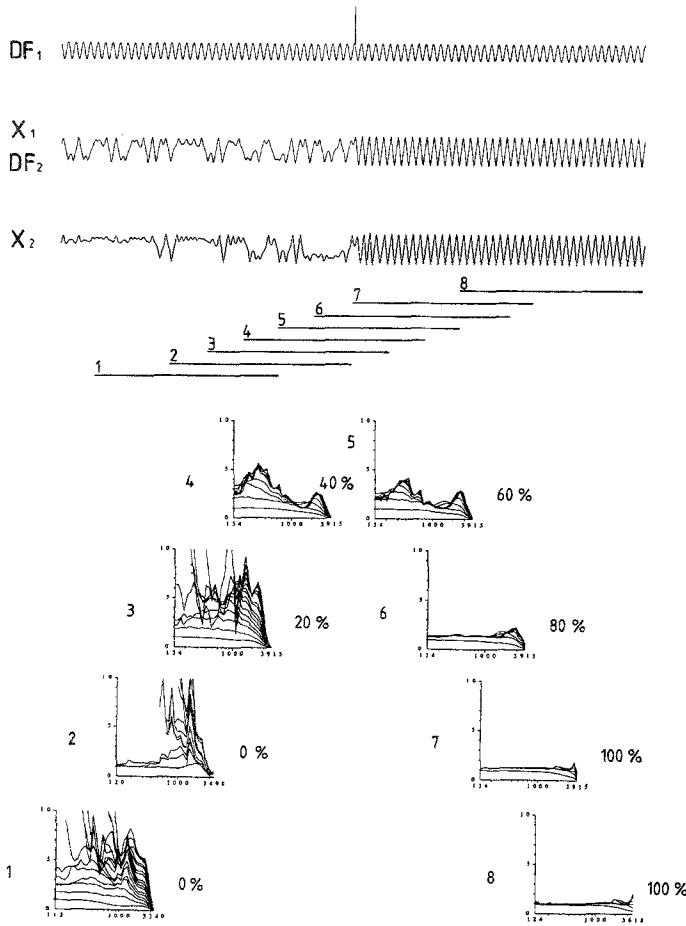


Figure App-1. Cascade of Duffing equations (both $(\delta, \gamma, \omega) = (0.15, 0.3, 1)$). Upper trace (DF_1) presents a signal used as the driving force for the first Duffing equation (the $\gamma \cos \omega t$ term in figure 1). In the middle of DF_1 an extra pulse is visible, 'pushing' that system from the chaotic mode into the limit cycle mode, as reflected in the solution of the equation, which is the signal X_1 (second trace). This signal, X_1 , is used as the driving force for the second Duffing equation. Therefore, the same signal is also denoted as DF_2 . The solution of the second equation is signal X_2 . D_2 analysis was performed on the signal X_2 using 8 partly overlapping epochs marked 1-8. Each epoch contained 5121 samples and covered 24 periods during the limit cycle mode (corresponding to an epoch of approximately 10 seconds of a 3 per-second spike-and-wave signal). The right tip of the abscissa of each D_2 -plot corresponds with the largest difference between all amplitudes of the samples of the epoch. The range of the ordinate of each D_2 -plot is from 0 to 10.

lyzed signals learned us that a general, "practical" recipe for a delay choice was not a simple matter while the pilot study taught us that the results using auto-scaled or fixed delays are not much different. This inspired us to follow the simpler recipe of choosing the fixed delay range of

20-300 ms for all signals and a fixed value for the Theiler correction (150 ms). (To be very precise: for embedding 1, 2, ..., 17 we used respectively 0, 112, 56, 84, 28, 98, 14, 70, 42, 105, 7, 91, 21, 77, 35, 63, and 49 sample distances of 2.7 ms each, resulting in delays of 0, 306.0, 153.0, 229.5, 76.5, 267.8, 38.3, 191.3, 114.8, 286.9, 19.1, 248.6, 57.4, 210.4, 95.6, 172.1, 133.9 ms.)

B: D_2 plots of a transition in the dynamics

A transition was created by making use of the Duffing system as presented in figure 1 of the main text (also $(\delta, \gamma, \omega) = (0.15, 0.3, 1)$). Since it is possible to generate limit cycle behavior (figure 1B) and chaotic dynamics (figure 1C) for one and the same set of values for the parameters (using different initial conditions) it is also possible to induce a transition from one mode to another without changing the parameters. One can begin in the chaotic mode and induce a transition to the limit cycle by applying an extra 'jolt' on top of the constant sinusoidal external driving force. Such a transition simulates the onset of an epileptic seizure, i.e., a transition from a complex to a more simple dynamics. However, it should be kept in mind that, when compared with ongoing, non-epileptiform EEG activity, D_2 of the chaotic mode is rather small. We, therefore, created a slightly more realistic simulation of the transition to an epileptic seizure as follows. We took the output of the previous situation and used it as driving force for a second Duffing "machine". A cascade of Duffing 'machines' is not so much related to epilepsy but in this way we obtained a transition from a really high-dimensional system to very low-dimensional one as occurs at seizure onset. Figure App-B-1 shows a gradual change, from a very high-dimensional D_2 -plot to one corresponding to a limit cycle. Furthermore, we note a 'mixed' D_2 -plot for transitions occurring between 20% and 80% of the total epoch duration only.

C: Example of a recurrence plot

In figure App-C-1 we show an example of a recurrence plot which reflects various dynamical aspects of signals that one may come across in practice all in one plot.

A signal was generated with the Duffing equation $((\delta, \gamma, \omega) = (0.15, 0.3, 1))$ showing, a transition from chaotic to limit cycle behavior in the middle. As in Appendix B, the transition was induced by an extra "jolt" on top of the periodic driving force. One may notice the following features:

- i. a striking discriminating power of the recurrence plot between the two types of behavior as reflected by the asymmetry between the left and right (upper and lower) half of the figure.

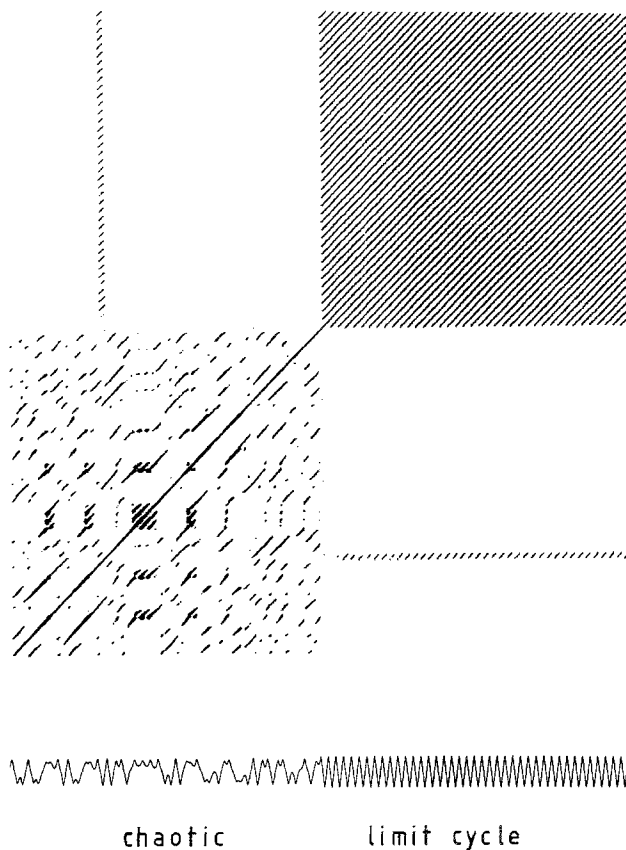


Figure App-2. A recurrence plot of a signal generated with the Duffing equation ($(\delta, \gamma, \omega) = (0.15, 0.3, 1)$). The solution of the equation changed in the middle of the epoch from chaotic to limit-cycle behavior, induced by adding a single pulse to the $\gamma \cos \omega t$ term.

- ii. periodic behavior results in stripes parallel to the diagonal at regular distances.
- iii. the chaotic behavior results in stripes of limited length. The smaller the largest Lyapunov exponent, the larger the (average) length of the stripes.

It is of importance is that the parts of the recurrence plots that correspond to the two different modes of behavior emerges as disjunct areas in the plot: the two off-diagonal quadrants are (almost) white. They are not completely white because during the chaotic mode a short lasting period of limit cycle like behavior occurs. The stripes in the off-diagonal quadrants reflect the correspondence of this behavior with that during the second half of the signal.

Short lasting transients in a signal, e.g., epileptiform spikes, are reflected as empty (white) horizontal and vertical stripes (crosses) across the whole plot. Examples of this may be found in figure 8A during phase I and II, in particular during phase I.

List of abbreviations

In the text:

ADC	analog to digital converter
CPS	complex partial seizure
ECoG	electro corticogram
EEG	electroencephalogram
FIR	finite impulse response (filter)
LGRP	linear Gaussian random process
log	logarithm with base 10
MTLE	mesial temporal lobe epilepsy
PCM	pulse code modulation
SCECoG	subchonic electro corticogram
SEEG	stereoelectroencephalogram
TLE	temporal lobe epilepsy
QEEG	quantitative EEG (analysis)

Electrodes:

ATL, ATR	anterior temporal left, - right
MTL, MTR	mid temporal left, - right
PTL, PTR	posterior temporal left, - right
AML, AMR	amygdala left, - right
HCL, HCR	hippocampus left, - right
G1	input amplifiers common reference electrode
G2	current-source electrode for compensating potential changes of G1

Epochs:

i	interictal
P	pre-ictal
S	seizure

Mathematical symbols:

$C(r,m)$	correlation integral
D_2	correlation dimension
h	Heaviside or step function
d	distance between two vectors (maximum norm)
k	largest delay
K_2	correlation entropy
log	logarithm with base 10
m	embedding dimension
N	number of (reconstructed) vectors in phase space
v	sampling frequency
T	time-window for the 'Theiler correction'
r	radius of a sphere in phase space
$\vec{V}_m(i)$	(reconstructed) vector in m -dimensional phase space
W,T	number of samples and time span of the window for the "Theiler correction"
x_i	sample i of the time series

Duffing equation:

t	time
x, \dot{x}, \ddot{x}	position, velocity and acceleration of the beam
δ	friction coefficient
γ	amplitude of the driving force
ω	angular frequency of the driving force

References

- Achermann, P., Hartmann, R., Gunzinger, A., Guggenbuhl, W. and Borbély, A.A. All-night sleep EEG and artificial stochastic control signals have similar correlation dimensions. *Electroenceph. clin. Neurophysiol.*, 1994, 90: 384-387.
- Albano, A.M., Muench, J., Schwartz, C., Mees, A.I., and Rapp, P.E. Singular-value decomposition and the Grassberger-Procaccia algorithm. *Phys. Rev. A* 1988, 38, 3017-3026.
- Babloyantz, A. and Destexhe, A. Low dimensional chaos in an instance of epilepsy. *Proc. Nat. Acad. Sci. (USA)*, 1986, a3: 3513-3517.
- Blinowska, K.J. and Malinowski, M. Non-linear and linear forecasting of the EEG time series. *Biol. Cybern.*, 1991, 66: 159-165.
- Brekelmans, G.J.F., van Emde Boas, W., Velis, D.N., van Huffelen, A.C., Debets, R.M.Ch. and van Veelen, C.W.M. Mesial temporal versus neocortical temporal lobe seizures: demonstration of different electroencephalographic spreading patterns by combined use of subdural and intracerebral electrodes. *J. Epilepsy*, 1995, 8: 308-320.
- Cerf, R., Ouldénoune, M., Ben Maati, M.L., El Ousdad, E.H. and Daoudi, A. Wave-separation in complex systems. Application to brain-signals. *J. of Biol. Phys.*, 1994, 19: 223-233.
- Delmas, A. and Pertuiset, B. *Cranio-cerebral topometry in man*. Paris, Masson, and Oxford, Blackwell Scientific Publications, 1959.
- Diks, C., van Houwelingen, J.C., Takens, F. and DeGoede, J. Reversibility as a criterion for discriminating time series. *Phys. Lett. A*, 1995, 201: 221-228.
- Eckmann, J.P., Oliffson Kamphorst, S. and Ruelle, D. Recurrence plots of dynamical systems. *Europhys. Lett.*, 1987, 4 (9): 973-977.
- Elbert, T., Ray, W.J., Kowalik, Z.J., Skinner, J.E., Graf, K.E. and Birbaumer, N. Chaos and physiology: deterministic chaos in excitable cell assemblies. *Physiol Rev*, 1994, 74(1): 1-47.
- Frank, G.W., Lookman, T., Nerengerg, M.A.H., Essex, C., Lemieux, J. and Blume, W. Chaotic time series analyses of epileptic seizures. *Physica D*, 1990, 46: 427-438.
- Fraser, A.M. and Swinney, H.L. Independent coordinates for strange attractors from mutual information. *Phys. Rev.*, 1986, 33A: 1134-1140.
- Freeman, W.J.. *Societies of Brains: A Study in the Neuroscience of Love and Hate*. Lawr. Erlb. Assoc.Publ., Hillsdale, New Jersey, 1995.
- Gotman, J. Automatic recognition of epileptic seizures in the EEG. *Electroenceph. clin. Neurophysiol.*, 1982, 54: 530-540.
- Gotman, J. Automatic seizures detection: improvements and evaluation. *Electroenceph. clin. Neurophysiol.*, 1990, 54: 530-540.
- Grassberger, P. and Procaccia, I. Measuring the strangeness of strange attractors. *Physica D*, 1983, 9: 189-208.
- Grassberger, P., Hegger, R., Kantz, H., Schaffrath, C. and Schreiber, Th. On noise reduction methods for chaotic data. *Chaos*, 1993, 3: 127-141.
- Guckenheimer, J. and Holmes, P. *Nonlinear oscillations, dynamical systems and bifurcations of vector fields*. Springer, Heidelberg, 1983.
- Hammel, S.M. A noise reduction method for chaotic systems. *Phys. Lett., A.*, 1990, 160: 421-428.
- Havstad, J.W. and Ehlers, C.L. Attractor dimension of nonstationary dynamical systems from small data sets. *Physical Review A*, 1989, 39: 845-853.
- Hayashi, H. and Ishizuka, S. Chaotic responses of the hippocampal CA3 region to a mossy fiber stimulation in vitro. *Brain Res.*, 1995, 686(2): 194-206.
- Hernández, J.L., Valdés, J.L., Biscay, R., Jiménez, J.C. and Valdés, P. EEG predictability: properness of non-linear forecasting methods. *Int. J. Bio-Med. Comp.*, 1995, 38: 197-206.
- van der Heyden, M.J., Diks, C., Pijn, J.P.M. and Velis, D.N. Time reversibility of intracranial human EEG recordings in temporal lobe epilepsy. *Phys.Lett.A*, 1996, 216: 283-288.
- Iasemidis, L.D., Sackellares, J.C., Zaveri, H.P. and Williams, W.J. Phase space topography and the Lyapunov exponent of electrocorticograms in partial seizures. *Brain Topogr.*, 1990, 2: 187-201.
- Iasemidis, L.D., Barreto, A., Uthman, B.M., Roper, S., Sackellares, I.C.. Spatio temporal evolution of dynamical measures precedes onset of mesial temporal lobe seizures. *Epilepsia*, 1994, 35 (Suppl. 8): 133.
- Iasemidis, L.D., Principe, J.C., Czaplewski, J.M., Gilmore, R.L., Roper, S.N. and Sackellares, I.C. Spatiotemporal transition to epileptic seizures: a nonlinear dynamical analysis of scalp and intracranial EEG recordings. In: F.L. Silva, J.C. Principe and L.B. Almeida (Ed.), *Spatiotemporal Models in Biological and Artificial Systems*. IOS Press, Amsterdam, 1996: 81-88.
- Ishizuka, S. and Hayashi, H. Chaotic and phase-locked responses of the somatosensory cortex to a periodic medial lemniscus stimulation in the anesthetized rat. *Brain Res.*, 1996, 723: 46-60.
- Kaboudan MA, 1993. A complexity test based on the correlation integral. *Phys. Lett. A* 181: 381-386.
- Kantz H and Schreiber T. Dimension estimates and physiological data. *Chaos*, 1995, 5 (1): 143-154.
- Kaplan, D.T. and Glass, L. Direct test for determinism in a time series. *Phys. Rev. letters*, 1992, 68: 427-430.
- Lehnertz, K and Elger, C.E. Spatio-temporal dynamics of the primary epileptogenic area in temporal lobe epilepsy characterized by neuronal complexity loss. *Electroenceph. clin. Neurophysiol.*, 1995, 95: 108-117.
- Lieb, J.P., Dasheiff, R.M. and Engel Jr, J. Role of the frontal lobes in the propagation of mesial temporal lobe seizures. *Epilepsia*, 1991, 32(6): 822-837.
- Lopes da Silva, F.H., Witter, M.P., Boeijinga, P.H. and Lohman, A.H.M. Anatomic organization and physiology of the limbic cortex. *Phys. Rev.*, 1990, 70(2): 453-511.
- Lopes da Silva, F.H. and Pijn, J.P.M. Epilepsy: network models of generation. In: M.A. Arbib (Ed.), *The Handbook of Brain Theory and Neural Networks*. The MIT Press, Massachusetts, USA, 1995: 367-369
- Lopes da Silva F. H., Pijn J.P.M. and Velis D.N. Signal processing of EEG: evidence for chaos or noise. An application to seizure activity in epilepsy. In: *Advances in Processing and Pattern Analysis of Biological Signals*. Edited by I. Gath and G.F. Inbar. Plenum Press, New York, 1996.
- Lopes da Silva, F.H., Pijn, J.P.M., Velis, D. and Nijssen, P.C.G.

- Alpha rhythms: noise, dynamics and models. In: E. Basar, R. Hari, F.H. Lopes da Silva and M. Schürmann (Ed.), *Alpha Activity: Cognitive and Sensory Behaviour*, Boston, In Press.
- Muhlcnickel, W., Rendtorff, N., Kowalik, J., Rockstroh, B., Miltner, W. and Elbert, T. Testing the determinism of EEG and MEG. *Integrative Physiological and Behavioral Science*, 1994, 29: 262-269.
- Müller-Gerking, J., Martinerie, J., Neuenschwander, S., Pezard, L., Renault, B. and Varela, F.J. Detecting non-linearities in neuro-electrical signals: a study of synchronous local field potentials. *Physica D*, 1996, 94: 65-91.
- van Neerven, J.M.A.M. Determination of the correlation dimension from a time series, applications to rat EEGs: sleep, theta rhythm and epilepsy. Master's thesis. Dept. Exp. Zoology, University of Amsterdam, 1987.
- Osborne, A.R., Kirwan Jr, A.D., Provenzale, A. and Bergamasco, L. A Search for chaotic behavior and mesoscale motions in the pacific ocean. *Physica D*, 1986, 23: 75-83.
- Osborne, A.R. and Provenzale, A. Finite correlation dimension for stochastic systems with power-law spectra. *Physica D*, 1989, 35: 357-381.
- Palus, M. Testing for Nonlinearity in the EEG. Technical report CCSR-92-16, Center for Complex Systems Research, University of Illinois at Urbana-Champaign, 1992.
- Pezard, L., Martinerie, J., Müller-Gerking, J., Varela, F.J. and Renault, B. Entropy quantification of human brain spatio-temporal dynamics. *Physica D*, 1996, 96: 344-354.
- Pijn, J.P.M. Quantitative evaluation of EEG signals in epilepsy; nonlinear associations, time delays and nonlinear dynamics. Ph.D. thesis, Rodopi, Amsterdam, 1990.
- Pijn, J.P.M., van Neerven, J., Noest, A., Lopes da Silva, F.H. Chaos or noise in EEG signals: dependence on state and brain site. *Electroenceph. clin. Neurophysiol.*, 1991, 79: 371-381.
- Pijn, J.P.M., Velis, D.N., van Emde Boas, W. and Lopes da Silva, F.H. Determination of seizure onset by means of chaos theory analysis of EEG records. *Epilepsia, suppl.*, 1992, 33: 64.
- Pradhan, N. and Narayana Dutt, D. A nonlinear perspective in understanding the neurodynamics of EEG. *Comput. Biol. Med.*, 1993, 23: 425-442.
- Prichard, D. and Theiler, J. Generating surrogate data for time series with several simultaneously measured variables. *Phys. Rev. Lett.*, 1994, 73: 951-954.
- Pritchard, W.S. and Duke, D.W. Measuring chaos in the brain: a tutorial review of nonlinear dynamical EEG analysis. *Int. J. Neurosci.*, 1992, 67: (1-4): 31-80.
- Provenzale, A., Smith, L.A., Vio, R. and Murate, G. Distinguishing between low-dimensional dynamics and randomness in measured time series. *Physica D*, 1992, 58: 31-49.
- Rapp, P.E. A guide to dynamical analysis. *Integr. Phys. and Behav. Sc.*, 1994, 29: 311-327.
- Rapp, P.E., Albano, A.M., Schmah, A.M. and Farwell, L.A. Filtered noise can mimic low-dimensional chaotic attractors. *Phys. Rev. E*, 1993, 47: 2289-2297.
- Rapp, P.E., Albano, A.M., Zimmerman, I.D. and Jimenez-Montaño, M.A. Phase-randomized surrogates can produce spurious identifications of non-random structure. *Phys. Lett. A*, 1994, 192: 27-33.
- Rombouts, S.A.R.B., Keunen, R.W.M. and Stam, C.J. Investigation of nonlinear structure in multichannel EEG. *Phys. Lett. A*, 1995, 202: 352-358.
- Schiff, S.J. and Chang, T. Differentiation of linearly correlated noise from chaos in a biologic system using surrogate data. *Biol. Cybern.*, 1992, 67: 387-393.
- Skarda, C.A. and Freeman, W.J. How brains make chaos in order to make sense of the world. *Behav. Brain Sci.*, 1987, 10: 161-195.
- Soong, A.C.K. and Stuart, C.I.J.M. Evidence of chaotic dynamics underlying the human alpha-rhythm electroencephalogram. *Biol Cybern.*, 1989, 62: 55-62.
- Takens, F. Detecting strange attractors in turbulence. In: *Dynamical Systems and Turbulence*, Warwick 1980. *Lecture Notes in Mathematics*, 1981, 898: 366-381.
- Takens, F. Detecting nonlinearities in stationary time series. *Int. J. Bifurc. Chaos*, 1993, 3(2): 241-256.
- Theiler, J. Spurious dimension from correlation algorithms applied to limited time-series data. *Phys. Rev. A*, 1986, 34: 2427-2432.
- Theiler, J. On the evidence for low-dimensional chaos in an epileptic electroencephalogram. *Physics Letters A*, 1995, 196: 335-341.
- Theiler, J., Eubank, S., Longtin, A., Galdrikian, B. and Doynne Farmer, J. Testing for nonlinearity in time series: the method of surrogate data. *Physica D*, 1992A, 58: 77-94.
- Theiler, J., Galdrikian, B., Longtin, A., Eubank, S. and Farmer, J.D. In: M. Casdagli and S. Eubank (Ed.), *Nonlinear Modeling and Forecasting*. Addison-Wesley, Reading, MA, 1992B.
- Theiler, J. and Rapp, P.E. Re-examination of the evidence for low-dimensional nonlinear structure in the human electroencephalogram. *Electroenceph. clin. Neurophysiol.*, 1996, 98: 213-223.
- Townsend III, J. B. and J. Engel Jr, J. "Clinicopathological correlations of low voltage fast and high amplitude spike and wave mesial temporal stereoencephalographic ictal onsets." *Epilepsia*, 1991, 32(3): 21.
- van Veelen, C.W.M., Debets, R.M.Chr., Van Huffelen, A.C., Van Emde Boas, W., Binnie, C.D., Storm van Leeuwen, W., Velis, D.N., van Dieren, A. Combined use of subdural and intracerebral electrodes in preoperative evaluation of epilepsy. *Neurosurgery*, 1990, 26: 93-101.
- Wadman, W.J., Jota, A.J.A., Kamphuis, W. and Somjen, G.G. Current source density of sustained potential shifts associated with electrographic seizures and with spreading depression in rat hippocampus. *Brain Research*, 1992, 570: 85-91.